Advances in Nano Research, *Vol. 11, No. 4 (2021) 405-422*
https://doi.org/10.12989/anr.2021.11.4.405

Free vibration of porous FG nonlocal modified couple nanobeams via a modified porosity model

Emad E. Ghandourah[1], Haitham M. Ahmed[2], Mohamed A. Eltaher*[3,4], Mohamed A. Attia[4] and Azza M. Abdraboh[5]

[1]*Nuclear Engineering Dept., Faculty of Engineering, King Abdulaziz University, P.O. Box 80204, Jeddah 21589, Saudi Arabia*
[2]*Mining Engineering Dept., Faculty of Engineering, King Abdulaziz University, Jeddah 21589, Saudi Arabia*
[3]*Mechanical Engineering Department, Faculty of Engineering, King Abdulaziz University, P.O. Box 80204, Jeddah, Saudi Arabia*
[4]*Mechanical Design & Production Department, Faculty of Engineering, Zagazig University, P.O. Box 44519, Zagazig, Egypt*
[5]*Physics Department, Faculty of Science, Benha University, Benha, Egypt*

(*Received June 12, 2021, Revised August 14, 2021, Accepted August 15, 2021*)

Abstract. This paper explores the size–dependent vibration response of porous functionally graded (FG) micro/nanobeams based on an integrated nonlocal-couple stress continuum model (NLCS). The mutual effect of the microstructure local rotation and nonlocality are modelled using the modified couple stress theory and Eringen nonlocal elasticity theory, respectively, into the classical Euler–Bernoulli beam model. All the material properties of the bulk continuum including the microstructure material length scale parameter (MLSP) are assumed to be graded along the thickness according to a power law. For the first time, the effect of the porosity and voids on the modulus of elasticity and MLSP is taken as a ratio of the mass density with porosity-to-that without porosity. Accounting for the physical neutral axis concept and generalized elasticity theory, Hamilton's principle is utilized to formulate the equations of motion and boundary conditions for the FG porous micro/nanobeams. The analytical solution using Navier method is applied to solve the governing equations and obtain the results. The impact of different parameters such as the gradation index, porosity pattern, porosity parameter, nonlocal parameter, and MLSP on the free vibration characteristics of simply supported FG nanobeams are presented discussed in detail. The current model is efficient in many applications used porous FGM, such as aerospace, nuclear, power plane sheller, and marine structures.
Keywords: analytical solutions; functionally graded structure; modified porosity model; nonlocal–modified couple stress model; size-dependent nanobeams

1. Introduction

During 1980s, Japanese's researchers had invited new advanced composite material that gradually changed smoothly through a certain spatial direction from metal phase to ceramic phase, and known as Functionally graded materials (FGMs), (Alshorbagy *et al*. 2011, Abo-Bakr *et al*. 2020a). These materials have enhanced mechanical properties, such as, rigidity, toughness, hardness, corrosion resistance, and thermal conductivity (Eltaher *et al*. 2018). Through the fabrication of FGM, microvoids are created and formed during sintering process because of the deviation in solidification temperatures of material constituents (Zhu *et al*. 2001). Sources of porosity formation include air bubbles entering the matrix material during melting or mixing processes and formation of water vapor on particles surfaces during solidification (Tapia *et al*. 2016). The porosity may be created by manufacturer in different applications, such as lightweight structures, biomedical systems, catalysts in electrochemical actuators and fuel cells, a piezoelectric ceramic graded actuator, porous titanium dioxide nano-layers, Hamed *et al*. (2019a).

Recently, many researchers and engineering are interesting in analyses of mechanical responses of FG porous structures with continuum mechanics theories. Kitipornchai *et al*. (2017) investigated the free vibration and buckling of FG porous beams reinforced by graphene platelets. Soliman *et al*. (2018) studied nonlinear transient response of natural gas pipe manufactured from FGM and subjected to internal pressure and unsteady temperature. Demirhan and Taskin (2019) investigated the bending and free vibration FG porous plate by using state space approach and four variable plate theory. Akbari *et al*. (2020) presented numerical solution for free vibration of sandwich porous FG cylindrical panels based on the linear poroelasticity theory of Biot. Akbaş *et al*. (2020a, b) developed a numerical finite element model to study the vibration response of FG porous 2D thick beam under the dynamic sine pulse load with and without viscoelastic support. Shariati *et al*. (2020) studied stability and dynamics of viscoelastic moving Rayleigh beams with an asymmetrical distribution of material parameters. Asemi *et al*. (2020) examined the static and dynamic responses of FG porous annular sector plates reinforced by graphene platelets by using finite element with a 4-node 2D element with 20 degrees of freedom. Hamed *et al*. (2020) illustrated

*Corresponding author, Professor,
E-mail: meltaher@kau.edu.sa
[a] Ph.D.
[b] Ph.D. Student

ISSN: 2287-237X (Print), 2287-2388 (Online)

the effect of axial load function on static stability of sandwich FG beams with porous core using higher order shear theory. Lyashenko *et al*. (2020) presented a dynamical model of the asymmetric actuator of directional motion based on power-law graded materials. Le *et al*. (2020) developed an analytical approach of nonlinear thermo-mechanical buckling of FG-CNTs composite laminated cylindrical shells under compressive axial load surrounded by elastic foundation. Ebrahimi *et al*. (2020) derived an exact solution of the buckling response of porous magneto-electro-elastic FG beam via different thermal loading functions. Bashiri *et al*. (2021) studied the free vibration of multilayered FG deep beams under thermal load by using 2D twelve-node plane element. Alnujaie *et al*. (2021a, b) studied the forced damped and undamped vibration responses of porous FG beam resting on viscoelastic foundation using 2D finite element and Newmark time integration technique. Abo-Bakr *et al*. (2021a) investigated the optimum weight of the FG beam structure subjected to variable compressive axial load under critical buckling constraints. Esen *et al*. (2021a) explored the vibration behavior of FG Timoshenko beam rested on elastic foundation with symmetric and sigmoidal material functions under the moving mass using a finite element analysis. Su *et al*. (2021) predicted the vibration response of FG porous piezoelectric deep curved beams resting on discrete elastic supports.

To consider the influence of size of nanostructures on the mechanical responses, various modified continuum theories are recommended, such as nonlocal elasticity, couple stress, strain gradient, nonlocal strain gradient (NSGT) and surface elasticity theories, Abdelrahman and Eltaher (2020). Reddy (2011) studied the nonlinear mechanical responses of Euler–Bernoulli and Timoshenko FG nanobeams including the microstructure influences. Farajpour *et al*. (2014) illustrated the surface effects on the mechanical characteristics of microtubule networks in living cells. Sedighi *et al*. (2014) investigated static and dynamic pull-in instability of multi-walled CNTs by he's iteration perturbation method. Ebrahimi and Salari (2015) illustrated the influence of thermal load on buckling and vibration characteristics of FG nonlocal Timoshenko nanobeams by using Navier type solution. Li and Hu (2016) explored analytically the nonlinear bending and vibration behaviors of NSGT FG nanobeams. Attia (2017) studied analytically the size-dependent mechanical responses of FG nanobeams using an integrated nonclassical continuum model. Attia and Abdelrahman (2018) considered the size influence on free vibration of FG viscoelastic nanobeams including the microstructure rotation and surface energy. Moory-Shirbani *et al*. (2018) studied experimental and mathematical analysis of a piezoelectrically actuated multilayered imperfect microbeam subjected to applied electric potential. Jena *et al*. (2019) studied the buckling loads and stability of SWCNTs nanobeam rested on Winkler foundation and exposed to a thermal environment considering the surface energy effect. Esmaeili and Tadi Beni (2019) examined the buckling and vibration behavior of FG flexoelectric nanobeam including the surface influences.

Hamidi *et al*. (2020) studied the forced axial vibration of NSGT nanobeam under axial harmonic moving and constant distributed forces. Attia and Mohamed (2020) studied the nonlinear thermal buckling and postbuckling of 2D-FGM tapered microbeams by using Reddy beam theory. Daikh *et al*. (2020) developed a comprehensive analysis to present the size and microstructure influences on static behavior of multilayer NSGT nanobeam reinforced by carbon nanotubes. Zine *et al*. (2020) explored the bending characteristics of graded porous plates employing a refined shear deformation theory. Abo-Bakr *et al*. (2020b, 2021b) studied the weight optimization of axially FG modified couple stress Timoshenko microbeams under buckling and vibration conditions. She (2020) and She *et al*. (2021) presented the Wave propagation and resonances of curved modified strain gradient theory microbeams reinforced with GNPs by utilizing Navier-type solution procedure. Alazwari *et al*. (2021) exploited modified couple stress and the modified Gurtin-Murdoch surface elasticity to include the microstructures influences on the static behavior of perforated microbeam. Abdelrahman *et al*. (2021a) exploited NSGT to analyze the dynamic behavior of perforated nanobeam structures under moving mass/load. Daikh *et al*. (2021a) studied bending of sigmoid FG sandwich nanoplates by using a novel NSGT quasi-3D plate theory. Daikh *et al*. (2021a) presented modified continuum model to examine the buckling and postbuckling of cross-ply single-walled carbon nanotube reinforced composite curved sandwich nanobeams subjected to thermal environment. Zhang *et al*. (2021) studied the nonlinear bending of FG curved nanobeams reinforced by CNTs in thermal environment by including effects of surface elastic theory and geometric nonlinearity. Esen *et al*. (2021b, c) studied the free vibration and buckling loads of FG NSGT nanobeams exposed to magnetic and thermal fields. Lu *et al*. (2021a, b) investigated free vibration, dynamic stability and postbuckling characteristics of geometrically imperfect FG-GPLRC modified strain gradient microtubes with different five distribution patterns. Koochi and Goharimanesh (2021) investigated the nonlinear oscillation of CNTs manufactured nano-resonator in the context of the nonlocal elasticity. Sedighi *et al*. (2021) reassessed flexure mechanics of nano-scale beams in the framework of the modified couple stress theory by applying a consistent variational scheme.

For a porous nanostructure including a size-dependent theories, Barati *et al*. (2017) studied forced vibration of porous metal foam NSGT nanoplates on elastic medium using a 4-variable plate theory and different porosity distributions functions. Eltaher *et al*. (2018) developed a modified implicit porosity model based on the apparent density to capture the real behavior of porous FG materials under static and dynamic behaviors. Dong *et al*. (2018) presented an analytical study to explore the buckling of spinning FG graphene reinforced porous nanocomposite cylindrical shells. Hamed *et al*. (2019) exploited nonlocal differential form of elasticity to include the size influence on the static deflection of porous FG Euler-Bernoulli nanobeam. Alipour and Shariyat (2019) developed a zigzag nonlocal model to study the deformation and stress

distribution of annular/circular 2D FG porous sandwich nanoplates with weak interfacial adhesions. Ebrahimi and Dabbagh (2019) exploited homogenization scheme to develop a novel porosity-based model and investigate a wave propagation in axially excited FG porous nanobeams. Aria and Friswell (2019) presented a nonlocal strain-driven FE model to analyze the free vibration and buckling behaviors of FG. Aria *et al*. (2019) exploited the previous model to investigate the thermo-elastic behavior of imperfect FG porous nanobeams rested on double-parameter elastic foundation. Ebrahimi *et al*. (2019) derived an exact solution of a thermo-mechanical vibration of porous curved FG NSGT nanobeams subjected to uniform thermal environmental conditions. Farzam and Hassani (2019) examined the mechanical behaviors of in-plane FG porous modified couple stress microplates by using isogeometric analysis. Emdadi *et al*. (2019) studied free vibration of annular sandwich plates with various FG porous modified couple stress nanoplate with carbon nanotubes reinforced composite. Esmaeilzadeh *et al*. (2019) utilized the NSGT to investigate the dynamic response of bi-2D FG porous nanoplates resting on elastic foundations. Kim *et al*. (2019) studied mechanical responses of modified couples stress FG porous microplates by using Navier solution technique. Sahmani and Madyira (2019) studied the size dependency in the nonlinear primary resonance of harmonic soft excited FG porous micro/nano-beams nanocomposite reinforced with graphene platelets. Karamanli and Aydogdu (2020) studied structural dynamics and stability of 2D-FG microbeams with two-directional porosity distribution and variable material length scale parameter. Ghandourh and Abdraboh (2020) developed nonlocal finite element model to study the influence of size-dependent on the dynamic behavior of FG porous nanobeam. Fenjan *et al*. (2020) utilized differential quadrature method for investigating free vibrations of porous FG micro/nano beams in thermal environments. Mohammadimehr and Meskini (2020) investigated the free and forced vibration of modified couple stress sandwich microplate with porous core layer and magnetoelectric face sheets. Fattahi *et al*. (2020) studied nonlinear secondary resonance of FG porous NSGT micro/nanobeams under periodic hard excitations by using the Galerkin method. Fan *et al*. (2021) studied thermal postbuckling response of porous FGM quasi-3D nanoplates based upon surface stress elasticity. Xu *et al*. (2021) presented the comparative analysis of the influence of nanovoids distribution associated with trigonometric functions on forced mechanical characteristics of FG curved nanobeams. Hadji and Avcar (2021) explored free vibration of porous FG nanobeams using nonlocal elasticity and hyperbolic shear deformation beam theory.

As seen from the literature survey, there is no study investigating the size-dependent vibration response of porous FG micro/nanobeam based on an integrated nonlocal-modified couple stress model. Therefore, this study aims to analyze the free vibration characteristics of porous FG micro/nanobeams considering the simultaneous effect of microstructure and nonlocal elasticity via the modified couple stress and Eringen's nonlocal elasticity theories, respectively, for the first time. Unlike the existing model, a modified porosity model is adopted to account for the implicit dependency of the material properties on the porosity content. Based on the generalized elasticity theory, the exact position of physical neutral axis is included. Different material properties such as the mass density, modulus of elasticity, Poisson's ratio, and material length scale parameter are graded along thickness direction as function of the gradient index and porosity. The nonlocal governing equations and associated boundary conditions are exactly derived using the generalized Hamilton's principle. Navier type solution is employed to derive an exact form for free vibration frequency of simply supported porous FG beams. Numerical results are presented and discussed to emphasize the effects of the porosity content, even and uneven distributions of porosities, gradient index, graded material length scale parameter, and the nonlocal parameter on the first three frequencies of porous FG nanobeams. The present results can be useful for the optimization of porous FG nanobeams and for validating other solution approaches.

2. Porous functionally graded materials

A FG nanobeam with length L, width b, and thickness h is considered accounting for random porosity distribution, with the rectangular coordinates system (x, y, z). The volume fraction of the constituent materials is graded along the beam thickness employing simple power law, which satisfies

$$\mathcal{v}_c(z) = \left(\frac{1}{2} + \frac{z}{h}\right)^K, \ \mathcal{v}_m(z) + \mathcal{v}_c(z) = 1, \quad 0 \le K < \infty \quad (1)$$

where the subscripts "m" and "c" denote the metallic and ceramic constituents, respectively, and K is the gradation power–law index via the thickness direction.

In the conventional porosity model (CPM), it is assumed that the porosity reduces the volume content of both metallic and ceramic phases equally, i.e., $\mathcal{v}_m$ and $\mathcal{v}_c$ by 0.5 p, where p denotes the porosity parameter, (Wattanasakulpong and Ungbhakorn 2014, Faleh *et al*. 2018, Jalaei and Civalek 2019, Ebrahimi *et al*. 2016, 2021). In this model, the effective material property $\mathcal{P}(z)$ of FG beam is introduced a modified rule of mixtures based on the even and uneven distributions of porosity, respectively, (Jalaei and Civalek 2019) as follows:

$$\mathcal{P}(z) = \mathcal{P}_m + (\mathcal{P}_c - \mathcal{P}_m)\mathcal{v}_c(z) - \frac{1}{2}p(\mathcal{P}_m + \mathcal{P}_c) \quad (1)$$

$$\mathcal{P}(z) = \mathcal{P}_m + (\mathcal{P}_c - \mathcal{P}_m)\mathcal{v}_c(z) - \frac{1}{2}p\left(1 - \frac{2|z|}{h}\right)(\mathcal{P}_m + \mathcal{P}_c) \quad (2)$$

where $\mathcal{P}_m$ and $\mathcal{P}_c$ denote, respectively, the material property of the metallic and ceramic phases. Although, Eqs. (2) and (3) are widely employed to evaluate the effective values of Young's modulus, mass density, Poisson's ratio, and other material properties, this relation reflects only the direct dependency on the mass density on the porosity but is not provide the dependency of other material properties such as the Young's modulus and Poisson's ratio on the mass density. In this regard, the modified porosity model

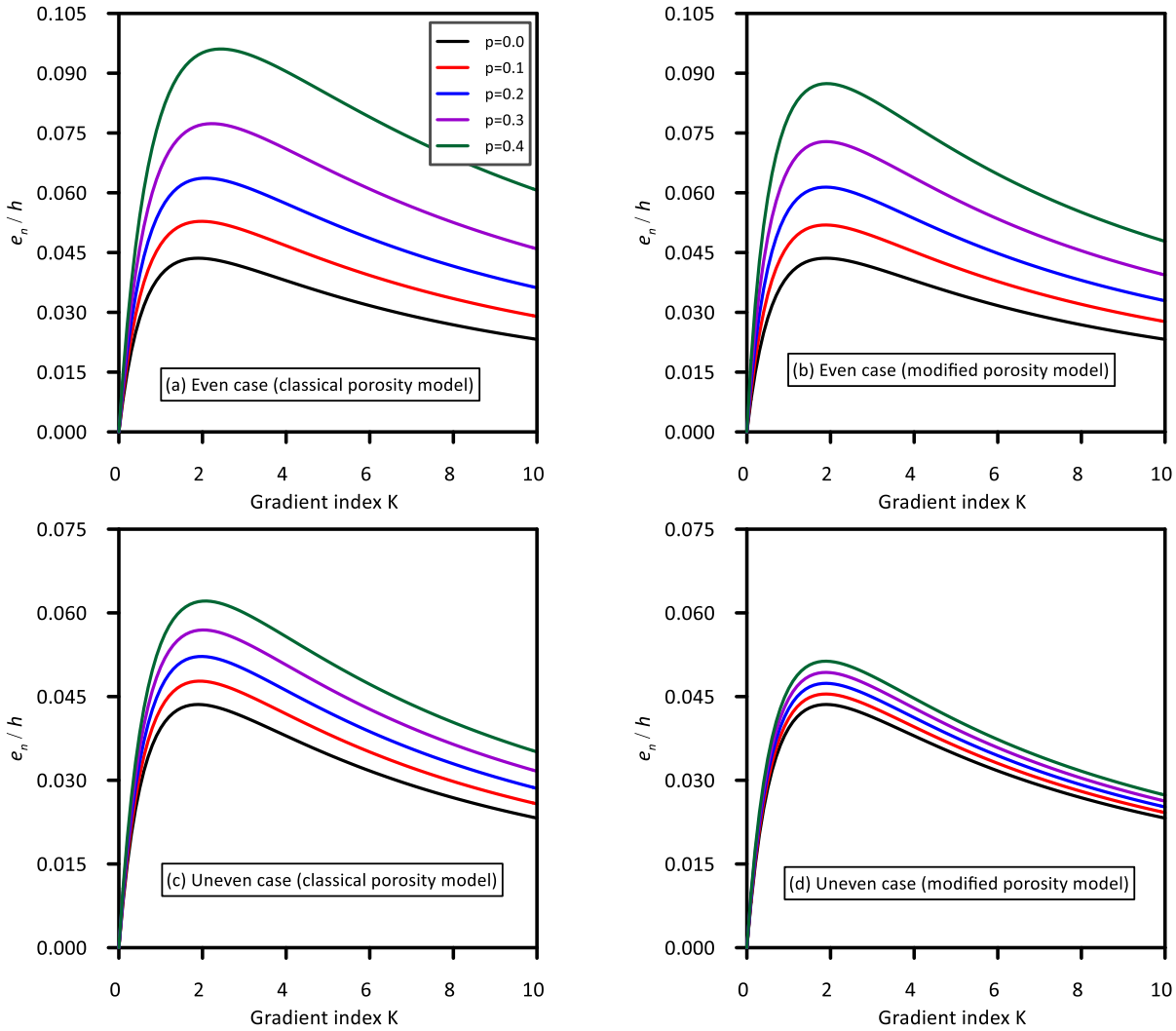

Fig. 1 Variation of the dimensionless position of the physical neutral axis of FG nanobeam with the gradient index based on classical and modified porosity models for even and uneven distributions of porosities

(MPM) proposed by Eltaher *et al*. (2018) is adopted to incorporates the porosity effect on the effective properties via the true and apparent densities of the material. In the MPM, the effective density can be approximated following Eqs. (2) and (3), for even and uneven distributed porosity, respectively, as

$$\rho(z) = \rho_m + (\rho_c - \rho_m)v_c(z) - \frac{1}{2}p(\rho_m + \rho_c) \tag{4}$$

$$\rho(z) = \rho_m + (\rho_c - \rho_m)v_c(z) - \frac{1}{2}p\left(1 - \frac{2|z|}{h}\right)(\rho_m + \rho_c) \tag{5}$$

The true mass density m_t and apparent mass density m_a are given by, Eltaher *et al*. (2018)

$$m_t = \int_0^L \int_A \rho(z)\, dAdx \quad \text{for } p = 0 \tag{6a}$$

$$\rho m_a = \int_0^L \int_A \rho(z)\, dAdx \quad \text{for } p > 0 \tag{6b}$$

Then, the effective modulus of elasticity (E), Poisson's ratio (v), microstructure material length scale parameter (l) can be approximately related to the true and apparent mass densities as follows:

For even distribution of porosities:

$$E(z) = E_m + (E_c - E_m)v_c(z) - \frac{1}{2}\frac{m_t - m_a}{m_t}(E_m + E_c) \tag{7a}$$

$$v(z) = v_m + (v_c - v_m)v_c(z) - \frac{1}{2}\frac{m_t - m_a}{m_t}(v_m + v_c) \tag{7b}$$

$$l(z) = l_m + (l_c - l_m)v_c(z) - \frac{1}{2}\frac{m_t - m_a}{m_t}(l_m + l_c) \tag{7c}$$

For uneven distribution of porosities:

$$E(z) = E_m + (E_c - E_m)v_c(z) - \frac{1}{2}\frac{m_t - m_a}{m_t}\left(1 - \frac{2|z|}{h}\right)(E_m + E_c) \tag{8a}$$

$$v(z) = v_m + (v_c - v_m)v_c(z) - \frac{1}{2}\frac{m_t - m_a}{m_t}\left(1 - \frac{2|z|}{h}\right)(v_m + v_c) \tag{8b}$$

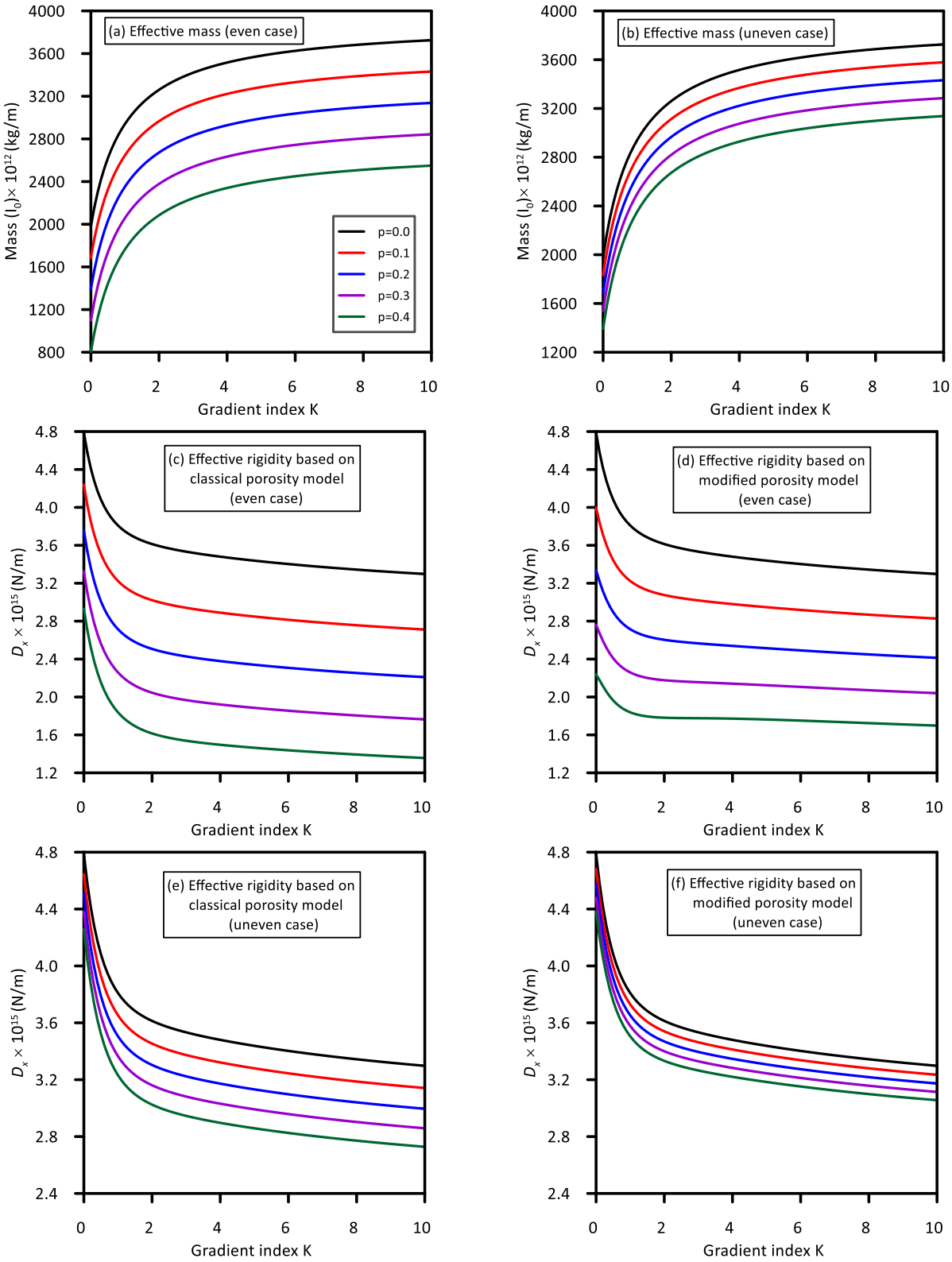

Fig. 2 Variation of the apparent mass density and rigidity of FG nanobeam with the gradient index based on classical and modified porosity models for even and uneven distributions of porosities

$$l(z) = l_m + (l_c - l_m)v_c(z) - \frac{1}{2}\frac{m_t - m_a}{m_t}\left(1 - \frac{2|z|}{h}\right)(l_m + l_c) \tag{8c}$$

Due to the material gradation along the thickness direction, the properties of FG nanobeam are unsymmetric about its middle surface and thus the physical neutral plane deviates from the geometric midplane. On the basis of

Table 1 Material properties of the FG nanobeam (stainless steel-alumina)

Material	Modulus of elasticity (GPa)	Mass density (kg/m^3)	Poisson's ratio
Steel	210	7800	0.30
Alumina	390	3960	0.24

generalized elasticity theory, the shift e_n between the physical neutral plane and midplane can be estimated as Eltaher *et al*. (2013), Simsek (2016), Attia (2018)

$$e_n = \frac{\int_h z[\lambda(z) + 2\mu(z)]\, dz}{\int_h [\lambda(z) + 2\mu(z)]\, dz} \tag{9}$$

Ignoring the effect of Poisson's ratio (one-dimensional elasticity), Eq can be written as

$$e_n = \frac{\int_h zE(z)\, dz}{\int_h E(z)\, dz} \tag{10}$$

Lamé's constants $\mu(z)$ and $\lambda(z)$ of continuum are given by

$$\begin{aligned} \mu(z) &= E(z)\frac{1}{2\big(1+\nu(z)\big)} \quad \text{and} \\ \lambda(z) &= E(z)\frac{\nu(z)}{\big(1+\nu(z)\big)\big(1-2\nu(z)\big)} \end{aligned} \tag{11}$$

In the present work, the FG nanobeam is assumed to be made of steel (metal constituent) and alumina (metal constituent), whose material properties are provided in Table 1, Fouda *et al*. (2017) and Eltaher *et al*. (2018). Also, the geometric parameters of the uniform nanobeam are L = 10^4 nm, b = 10^3 nm, and $h = L/20$, unless other values are mentioned.

The influence of the gradation index on the dimensionless location of physical neutral plane, i.e., e_n/h, of porous FG nanobeam is shown in Fig. 1 for both even and uneven distributions based on classical and modified porosity models. Increasing the gradient index K yields a significant rise in the distance e_n, with a maximum e_n reached at K^*. The value of K^* depends on the porosity parameter for CPM, whereas it is almost constant (K^*=1.9) for MPM. Also, it is noted that at a constant porosity parameter, the deviation e_n associated with the uneven type is always less than that associated with the even type and classical porosity model (CPM) gives a greater e_n compared with modified porosity model (MPM).

Fig. 2 shows the variations of the apparent mass (m_a) and the rigidity ($D_x = \int_{-0.5h-e_n}^{0.5h-e_n} \big(z^2 E(z)\big) dz$) of the nanobeam with the gradient index and porosity using both classical and modified porosity models for even and uneven distributions. It is depicted that increasing the gradient index shows an increase in the apparent mass and a decrease in the rigidity, which is attributed to rising the volume content of the metallic phase, which has higher mass density and lower modulus of elasticity, with increasing the gradient index. Based on both the classical and modified porosity model, the mass and rigidity of the nanobeam are reduced as the porosity parameter (b) increases in even and uneven distributions. The ratio of the predicted rigidity utilizing the MPM -to- that utilizing the CPM is about 0.9624 and 1.033 at K = 0.5 and 1.0383 and 1.05 at K = 2, for even and uneven cases, respectively.

3. Mathematical formulation

In the present study, Euler–Bernoulli beam theory is used to express the kinematics of nanobeam under consideration. The displacement components u and w along x and z directions, respectively, at any point of the beam, are given as, Alshorbagy *et al*. (2011)

$$\begin{aligned} u(x,z,t) &= -z_n \frac{\partial W(x,t)}{\partial x} \\ w(x,z,t) &= W(x,t) \end{aligned} \tag{12}$$

where $W(x,t)$ is the transverse displacement of the elastic center on the physical neutral axis at time t and $z_n = z - e_n$.

3.1 Review of the modified couple stress theory

In the context of the generalized linear elasticity theory combined with the modified couple stress theory (MCST) proposed by Yang *et al*. (2002) and Ma *et al*. (2008), the constitutive equations of the beam can be written as

$$\sigma_{ij} = 2\mu(z)\varepsilon_{ij} + \lambda(z)\varepsilon_{kk}\delta_{ij} \tag{13}$$

$$m_{ij} = 2l(z)^2\mu(z)\chi_{ij} \tag{14}$$

where σ_{ij} is the local–Cauchy stress vector and m_{ij} is the deviatoric part of the couple stress tensor and δ_{ij} is the Kronecker delta. The material length scale parameter (MLSP) "$l(z)$" is a measure of the influence of material microstructure, Mindlin (1963). In this study, the MLSP depends on both the gradient index and porosity parameter, for the first time. In Eqs. (6) and (7), the summation convention and standard index notation are implied, Latin and Greek indices run over, respectively, 1,2,3, and 1,2.

On the basis of the infinitesimal strain assumptions, the strain (ε_{ij}) and the symmetric curvature tensors (χ_{ij}) are given by the following relations, respectively, Yang *et al*. (2002) and Ma *et al*. (2008)

$$\varepsilon_{ij} = \frac{1}{2}\big(u_{i,j} + u_{j,i}\big) \tag{15}$$

$$\begin{aligned} \chi_{ij} &= \frac{1}{2}\big(\theta_{i,j} + \theta_{j,i}\big) \\ \theta_i &= \frac{1}{2}\varepsilon_{ijk}u_{k,j} \end{aligned} \tag{16}$$

in which, u_i and θ_i are, respectively, the components of the displacement and the rotation vector and ε_{ijk} denotes the permutation tensor. ε_{ij}, χ_{ij}, θ_i

Inserting Eq. (5) into Eqs. (8)-(10), one can obtain the components ε_{ij}, θ_i, and χ_{ij}, and then using Eqs. (6) and (7), the components of σ_{ij} and m_{ij} can be obtained, as follows:

$$\varepsilon_{xx}(t) = -z_n \frac{\partial^2 W(x,t)}{\partial x^2} \tag{17}$$

$$\theta_y(t) = -\frac{\partial W(x,t)}{\partial x}$$
$$\chi_{xy}(t) = -\frac{1}{2}\frac{\partial^2 W(x,t)}{\partial x^2} \tag{18}$$

$$\sigma_{xx} = -z_n[\lambda(z) + 2\mu(z)]\frac{\partial^2 W(x,t)}{\partial x^2}$$
$$\sigma_{yy} = \sigma_{zz} = -z_n\lambda(z)\frac{\partial^2 W(x,t)}{\partial x^2} \tag{19}$$

$$m_{xy} = -[l(z)^2\mu(z)]\frac{\partial^2 W(x,t)}{\partial x^2} \tag{20}$$

3.2 Review of the nonlocal constitutive relation

Based on Eringen nonlocal elasticity theory, Eringen (1983), the transformed differential nonlocal constitutive equation is

$$\sigma_{ij}^n - \eta\,\nabla^2\sigma_{ij}^n = \sigma_{ij}^l \tag{21}$$

where σ_{ij}^l and σ_{ij}^n represent, respectively, the components of local and the nonlocal stress tensors, η is the nonlocal parameter that measures the significance of the inter-atomic long-range force, i.e., $\eta = (e_0 a)^2$, where a denotes a material-dependent internal characteristic length and e_0 an experimental constant appropriate to each material. For isotropic FG nanobeam and in light of Eqs. (18)-(20), the nonlocal constitutive relations are as follows:

$$\sigma_{xx}^n - \eta\,\nabla^2\sigma_{xx}^n = \sigma_{xx}^l \equiv -z_n[\lambda(z) + 2\mu(z)]\frac{\partial^2 W(x,t)}{\partial x^2} \tag{22a}$$

$$\sigma_{yy}^n - \eta\,\nabla^2\sigma_{yy}^n = \sigma_{yy}^l \equiv -z_n\lambda(z)\frac{\partial^2 W(x,t)}{\partial x^2},\quad \sigma_{zz}^n = \sigma_{yy}^n \tag{22b}$$

$$m_{xy}^n - \eta\,\nabla^2 m_{xy}^n = m_{xy}^l \equiv -[l(z)^2\mu(z)]\frac{\partial^2 W(x,t)}{\partial x^2} \tag{22c}$$

3.3 Governing equation

The generalized Hamilton's principle states that

$$\delta\int_{t_1}^{t_2}(\mathbb{T} + \mathbb{W} - \mathbb{U})\,dt = 0 \tag{23}$$

in which, $\mathbb{U}$ is the strain energy of the bulk continuum incorporating the influence of microstructure, $\mathbb{T}$ is the kinetic energy, and $\mathbb{W}$ is the work done by the applied external loadings and couple moment. Since the present study concerns with free vibration response of nanobeams, thus $\mathbb{W} = 0$. Using Eqs. (17)-(20), the variation of the strain energy can be calculated as:

$$\delta\mathbb{U} = \frac{1}{2}\delta\int_0^L\int_A\left(\sigma_{ij}\varepsilon_{ij} + m_{ij}\chi_{ij}\right)dAdx \tag{24}$$

$$= \frac{1}{2}\delta\int_0^L\int_A\left(\sigma_{xx}\varepsilon_{xx} + 2m_{xy}\chi_{xy}\right)dAdx$$
$$\equiv \int_0^L -\left(M_x + Y_{xy}\right)\frac{\partial^2\delta W(x,t)}{\partial x^2}dx$$

in which, the stress resultants are defined as

$$M_x \equiv \int_A z_n\sigma_{xx}\,dA = -D_x\frac{\partial^2 W(x,t)}{\partial x^2} \tag{25a}$$

$$Y_{xy} \equiv \int_A m_{xy}\,dA = -S_{xy}\frac{\partial^2 W(x,t)}{\partial x^2} \tag{25b}$$

with

$$\begin{Bmatrix} D_x \\ S_{xy}\end{Bmatrix} \equiv \int_A \begin{Bmatrix} {z_n}^2\left(\lambda(z) + 2\mu(z)\right) \\ l(z)^2\mu(z)\end{Bmatrix} dA \tag{26}$$

The variation of the kinetic energy ($\mathbb{T}$) or Euler–Bernoulli nanobeam is given by

$$\delta\mathbb{T} = \frac{1}{2}\delta\int_0^L\int_A\rho(z)\left[\left(\frac{\partial u(x,t)}{\partial t}\right)^2 + \left(\frac{\partial w(x,t)}{\partial t}\right)^2\right]dAdx$$
$$= \int_0^L\left[\left(\mathrm{I}_2\frac{\partial^2 W(x,t)}{\partial x\partial t}\right)\frac{\partial^2\delta W(x,t)}{\partial x\partial t}\right.$$
$$\left. + \left(\mathrm{I}_0\frac{\partial W(x,t)}{\partial t}\right)\frac{\partial\delta W(x,t)}{\partial t}\right]\frac{\partial^2\delta W(x,t)}{\partial x\partial t}dx \tag{27}$$

The mass moments of inertia I_0 and I_2 are defined as follows:

$$\begin{Bmatrix}\mathrm{I}_0 \\ \mathrm{I}_2\end{Bmatrix} \equiv \int_A \rho(z)\begin{Bmatrix}1 \\ {z_n}^2\end{Bmatrix} dA \tag{28}$$

To this end, substituting Eqs. (24) and (28) into Eq. (26), proceeding the integration by parts, and specifying the coefficient of δw to zero, the following differential equation of motion with respect to the nonlocal stress resultants can be derived:

$$\mathrm{I}_2\frac{\partial^4 W}{\partial x^2\partial t^2} - \mathrm{I}_0\frac{\partial^2 W}{\partial t^2} + \left(\frac{\partial^2 M_x^n}{\partial x^2} + \frac{\partial^2 Y_{xy}^n}{\partial x^2}\right) = 0 \tag{29}$$

with the following nonclassical boundary conditions:

$$W = \bar{W} \quad \text{or} \quad -\mathrm{I}_2\frac{\partial^3 W}{\partial x\partial t^2} - \left(\frac{\partial M_x^n}{\partial x} + \frac{\partial Y_{xy}^n}{\partial x}\right) + \bar{V} = 0 \tag{30a}$$

$$\frac{\partial W}{\partial x} = \frac{\overline{\partial W}}{\partial x} \quad \text{or} \quad M_x^n + Y_{xy}^n - \bar{M} = 0 \tag{30b}$$

To formulate the derived equation of motion and associated boundary conditions in terms of the displacement components, employ the nonlocal differential elasticity theory and applying the conjugate differential operator $(1 - \eta\nabla^2)$ in Eq. (21) on the resultant moment (Eq. (25)), such that

$$M_x^n - \eta\frac{\partial^2 M_x^n}{\partial x^2} = M_x^l \equiv -D_x\frac{\partial^2 W(x,t)}{\partial x^2} \tag{31a}$$

$$Y_{xy}^n - \eta\frac{\partial^2 Y_{xy}^n}{\partial x^2} = Y_{xy}^l \equiv -S_{xy}\frac{\partial^2 W(x,t)}{\partial x^2} \tag{31b}$$

From Eqs. (31a) and (31b),

$$M_x^n + Y_{xy}^n = \eta\left(\frac{\partial^2 M_x^n}{\partial x^2} + \frac{\partial^2 Y_{xy}^n}{\partial x^2}\right) - D_e\frac{\partial^2 W(x,t)}{\partial x^2} \quad (32)$$

in which, $D_e = D_x + S_{xy}$. Substituting the second derivative of $(M_x^n + Y_{xy}^n)$ from Eq. (29) into Eq. (32) and then substitute into Eq. (29) gives the following six-order differential nonlocal equation of motion in terms of the displacement of porous FG Euler–Bernoulli nanobeam:

$$-\eta \mathrm{I}_2\frac{\partial^6 W}{\partial x^6 \partial t^2} + (\mathrm{I}_2 + \eta \mathrm{I}_0)\frac{\partial^4 W}{\partial x^2 \partial t^2} - \mathrm{I}_0\frac{\partial^2 W}{\partial t^2} - D_e\frac{\partial^4 W}{\partial x^4} = 0 \quad (33)$$

The corresponding nonlocal boundary conditions at $x = 0$ and $x = L$ are as follows:

$$W = \bar{W} \quad \text{or} \quad -\eta \mathrm{I}_2\frac{\partial^5 W}{\partial x^3 \partial t^2} + (\mathrm{I}_2 - \eta\, \mathrm{I}_0)\frac{\partial^3 W}{\partial x^2 \partial t} - D_e\frac{\partial^4 W}{\partial x^4} = \bar{V} \quad (34a)$$

$$\frac{\partial W}{\partial x} = \frac{\overline{\partial W}}{\partial x} \quad \text{or} \quad -\eta\, \mathrm{I}_2\frac{\partial^4 W}{\partial x^2 \partial t^2} + \eta\, \mathrm{I}_0\frac{\partial^2 W}{\partial t^2} - D_e\frac{\partial^2 W}{\partial x^2} = \bar{M} \quad (34b)$$

4. Analytical solution

The Navier solution procedure is adopted to analytically solve the derived equation of motion for free vibration of a simply supported porous FG nanobeam based on the nonlocal-modified couple stress theory. For simply supported ends, the nonlocal boundary conditions at are

$$W = \bar{W} \quad \text{and} \quad -\eta\, \mathrm{I}_2\frac{\partial^4 W}{\partial x^2 \partial t^2} + \eta\, \mathrm{I}_0\frac{\partial^2 W}{\partial t^2} - D_e\frac{\partial^2 W}{\partial x^2} = 0 \quad at\ x = 0, L \quad (35)$$

To satisfy the equation of motion given by Eq. (33) and the boundary conditions in Eq. (35), the displacement field can be assumed as, Reddy (2007)

$$W(x,t) = \sum_{m=1}^{\infty} \mathrm{W}_m \sin\left(m\pi\frac{x}{L}\right) e^{i\omega_m t} \quad (36)$$

where $i = \sqrt{-1}$, W_m are the unknown Fourier coefficients, and ω_m is the vibration natural frequency. Substitution of Eq. (36) into Eq. (33), the closed–form solution for the natural frequency of porous FG simply supported Euler-Bernoulli nanobeam can be obtained as:

$$\omega_m^2 = \frac{D_e \xi_m^4}{(1 + \eta\xi_m^2)(\mathrm{I}_0 + \xi_m^2 \mathrm{I}_2)}, \qquad \xi_m = \frac{m\pi}{L} \quad (37)$$

5. Numerical results and discussions

In this section, the influence of porosity content, porosity distribution, gradient index, and the material length scale parameter on the free vibration characteristic of a simply supported porous FG nanobeam is explored employing the developed nonlocal-couple stress model. There is no available data in the open literature for the microscale material properties on the basis of combining the nonlocal and modified couple stress theories and therefore, the material properties are assumed to be size-independent. Here, a porous FG nanobeam with the material properties provided in Table 1 and dimensions L=10000 nm, b=1000 nm, and $h = L/20$, unless other values are mentioned. Due to the lack of experimental data on porous FG materials, the nonlocal parameter is taken as 3×10^{-12} and the microstructure material length scale parameter $l(z)$ is modelled according to Eq. (8c) as a function of the gradient index and porosity content with $l_m = 0.4h$ and $l_c = 4l_m/3$. To explore the small scale effect, four different continuum models are employed; the classical model "CL" which ignores the contribution of both microstructure and nonlocality ($l_m = l_c = \eta = 0$), modified couple stress model "CS" which includes only the influence of microstructure via the MCST ($\eta = 0$), nonlocal elasticity model "NL" which incorporates the influence of nonlocal elasticity only ($l_m = l_c = 0$), and nonlocal elasticity-modified couple stress model "NLCS" which combines the influences of nonlocal elasticity and microstructure. All the forthcoming results are performed based on the modified porosity model (MPM). For convenience, the fundamental frequencies are presented as nondimensional as $\bar{\omega}_m = \omega_m L^2\sqrt{\rho_c A/E_c I}$.

The effect of the porosity content on the vibration of FG nanobeam is predicted based on the different continuum models, i.e., CL, CS, NL, and NLCS. Figures 4–6 show the variation of the dimensionless first three frequencies versus the porosity parameter at different values of the gradient index, considering both even and uneven patterns of porosity distribution. It is revealed that for pure ceramic (K=0), the even distribution of porosity yields higher frequencies compared with the uneven one, which is in accordance with the plots in Fig. 1. As the porosity parameter (p) increases, the predicted frequencies are significantly reduced for even case and are remarkably increased for the uneven case, depending on the value of the gradient exponent. It is seen that for CL and NL models of porous nanobeam with K=0, the increase in the porosity content of even type leads to a reduction in the frequencies till reaching a certain value, then the trend is reversed. This is because that in CS and NLCS models, the porosity content contributes to the material length scale parameter and thus reduces the beam rigidity. It is seen that for the first three frequencies, the highest values are obtained employing the CS model due to the significant increase in the beam rigidity, whereas the lowest values are obtained employing the NL model, due to the softening effect of nonlocal elasticity.

The effect of the gradient index on the predicted first three frequencies of simply supported porous FG nanobeam is demonstrated in Figs. 7-9, adopting different continuum models. The results are recorded with even and uneven distribution of porosity. It is depicted that the vibration response of the beam is remarkably influenced by varying

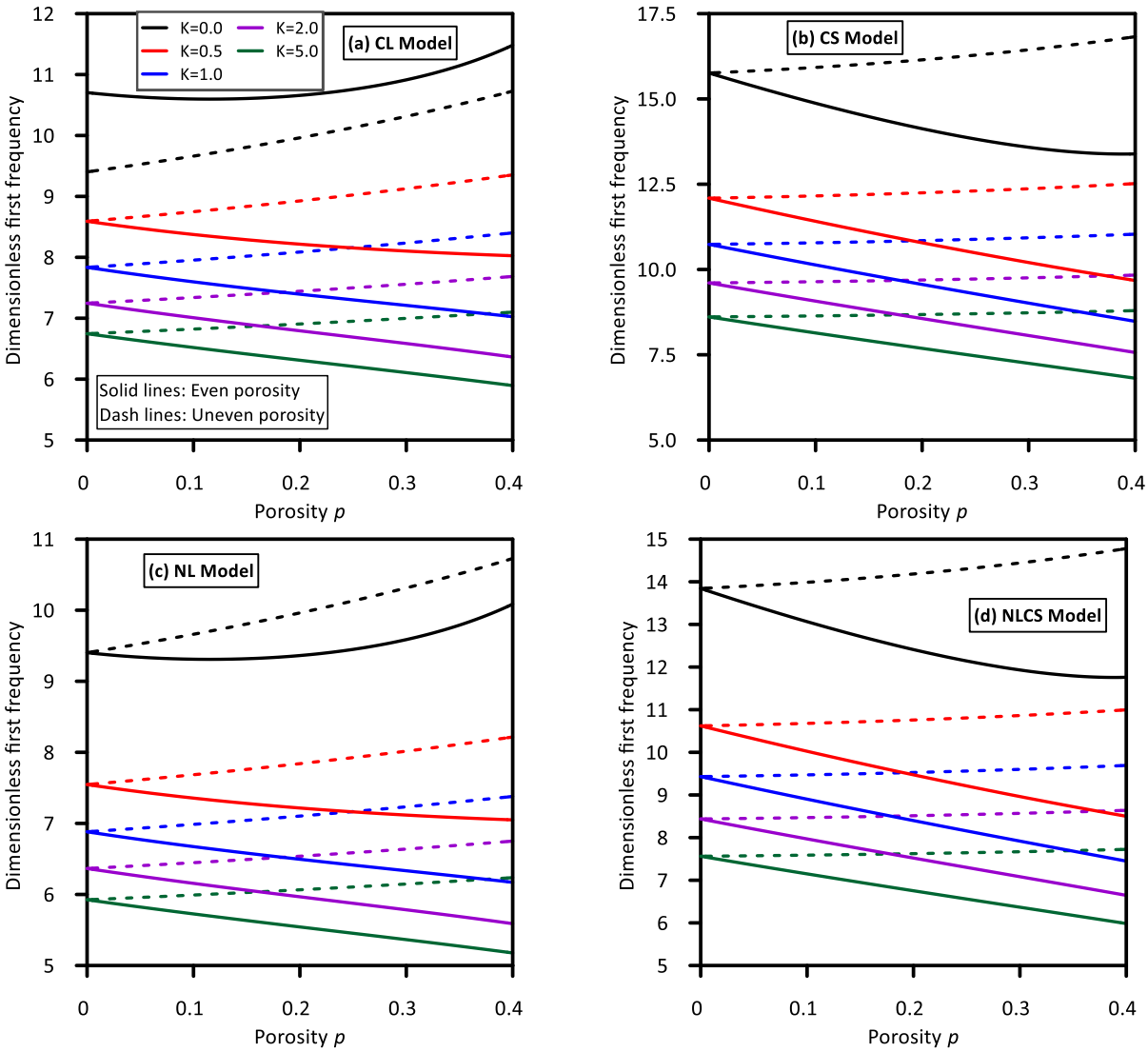

Fig. 3 Variation of the dimensionless first frequency with the porosity parameter using even and uneven porosity models and different gradient indices

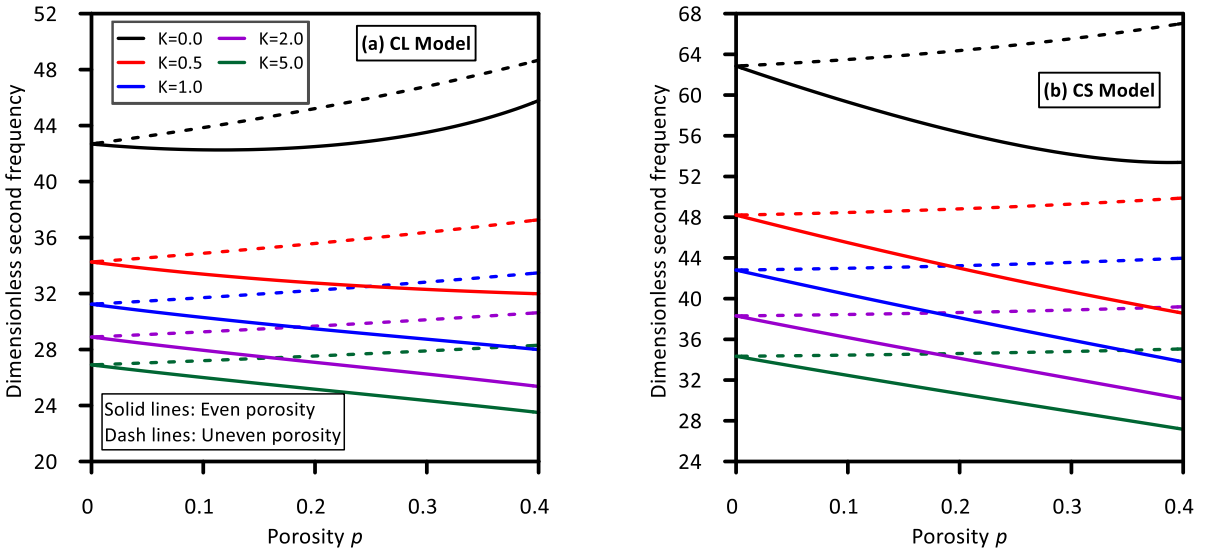

Fig. 4 Variation of the dimensionless second frequency with the porosity parameter using even and uneven porosity models and different gradient indices

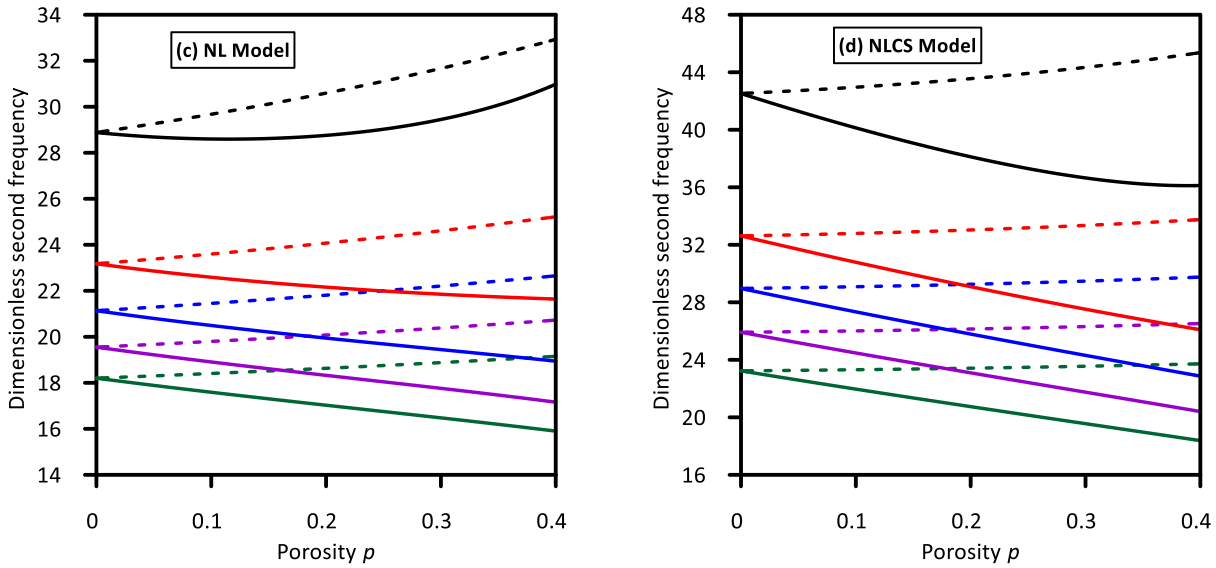

Fig. 4 Continued

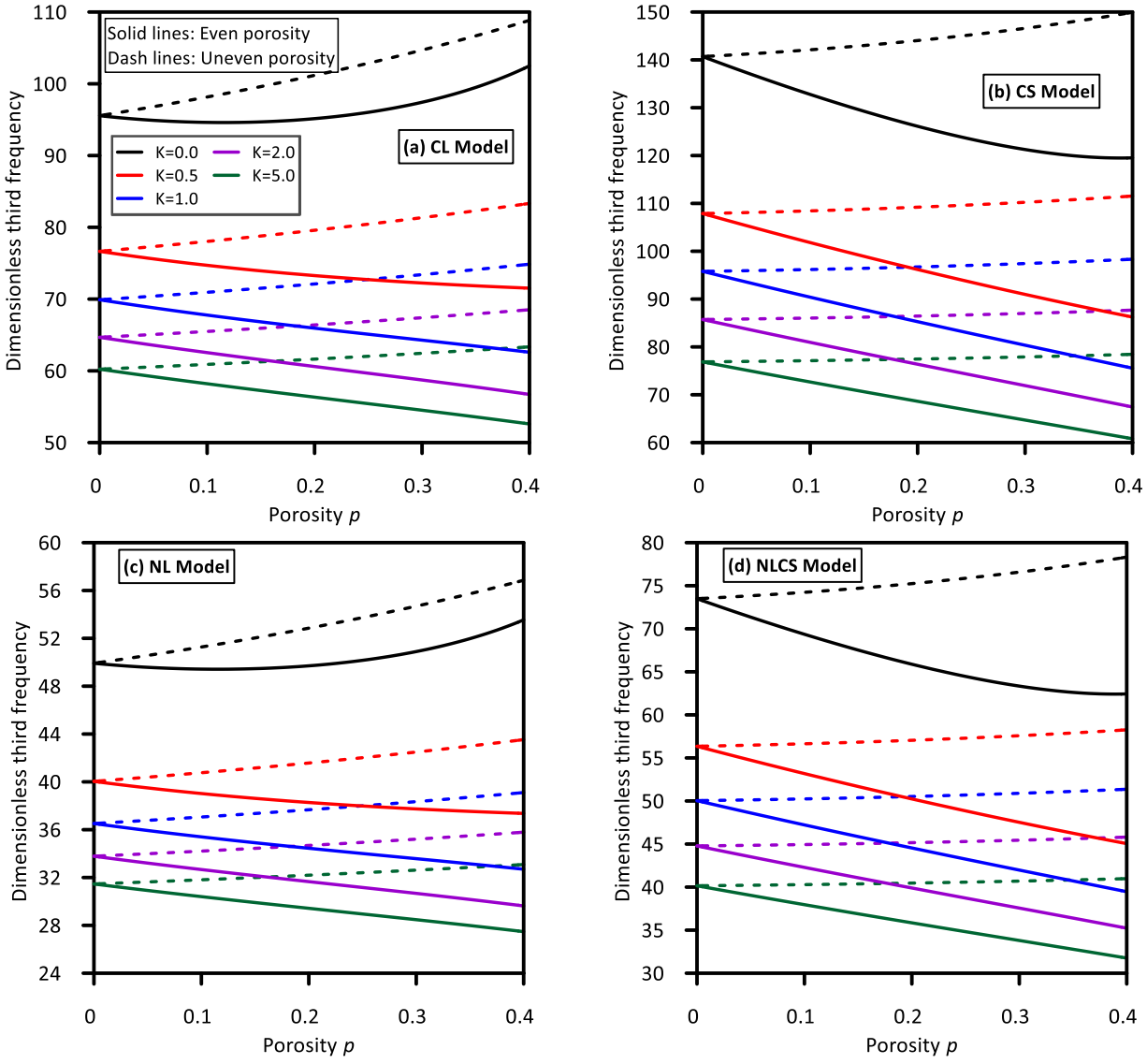

Fig. 5 Variation of the dimensionless third frequency with the porosity parameter using even and uneven porosity models and different gradient indices

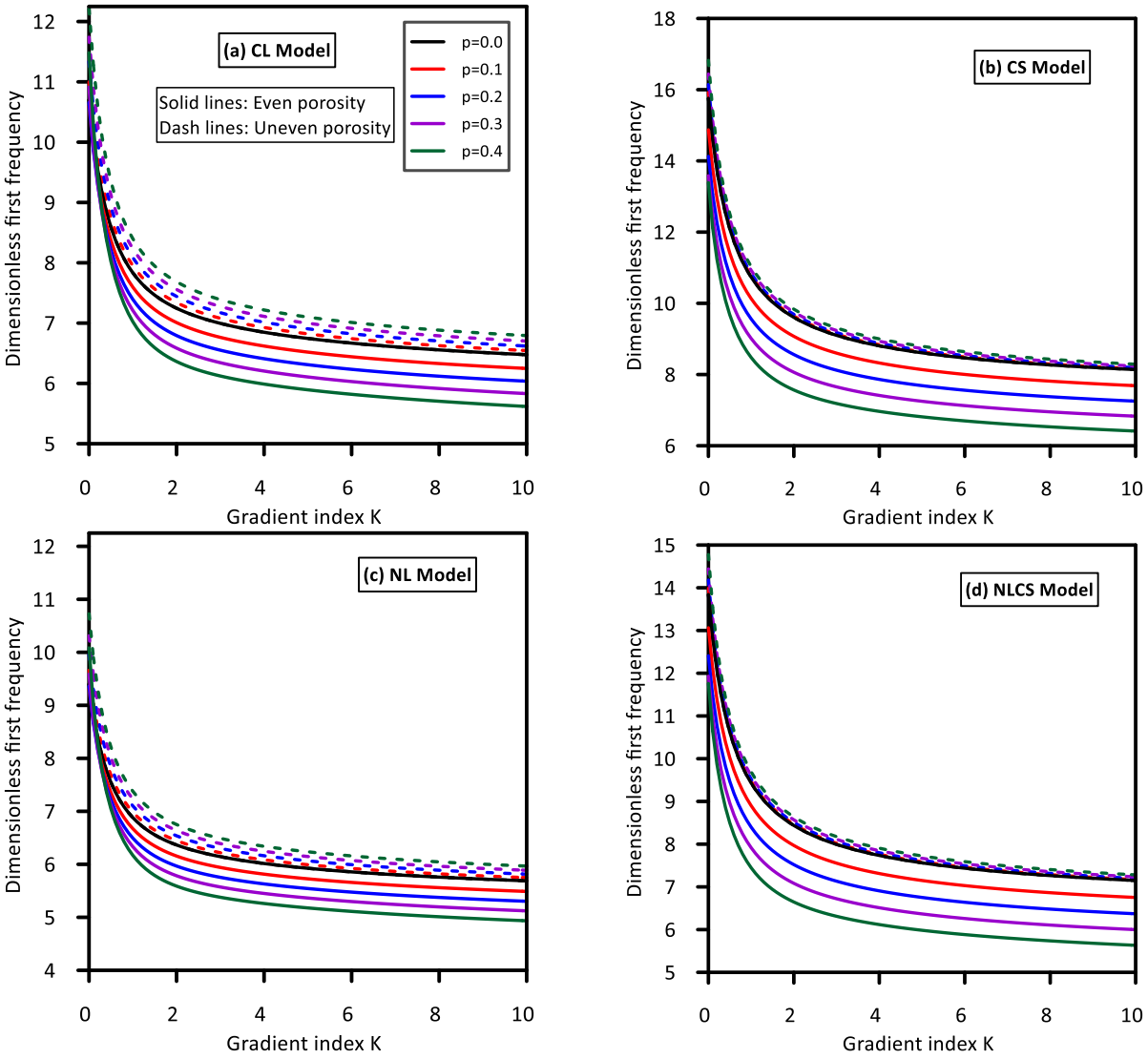

Fig. 6 Variation of the dimensionless first frequency with the gradient index at different porosities using even and uneven porosity models

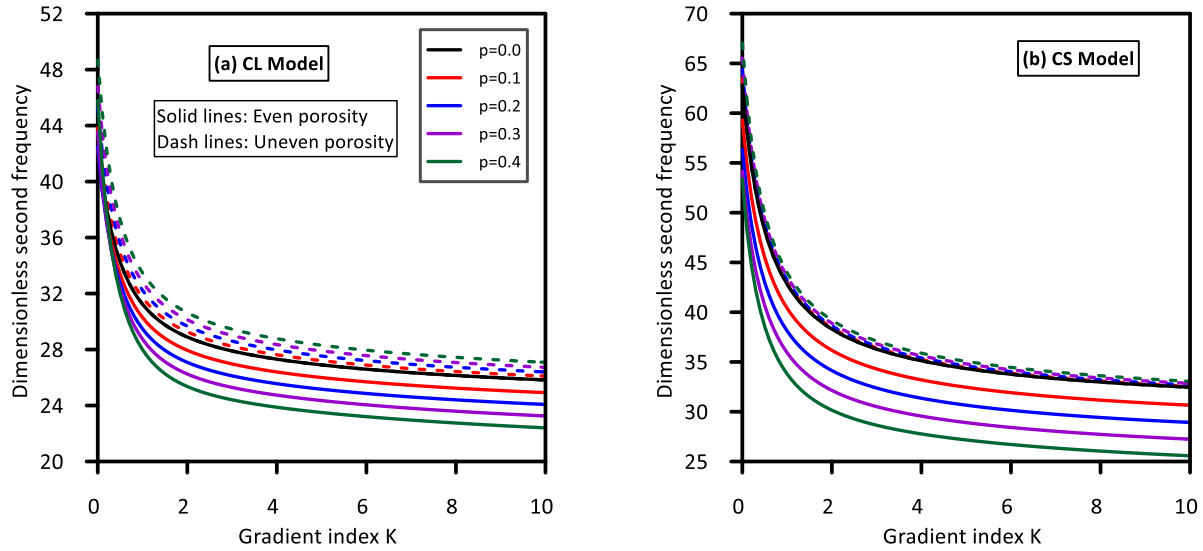

Fig. 7 Variation of the dimensionless second frequency with the gradient index at different porosities using even and uneven porosity models

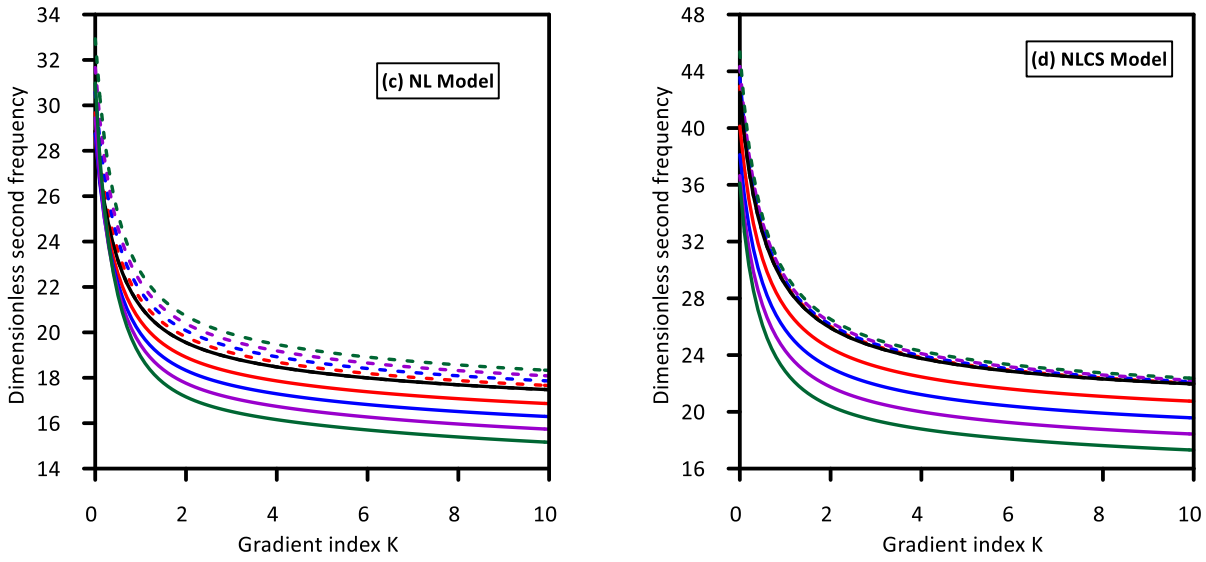

Fig. 7 Continued

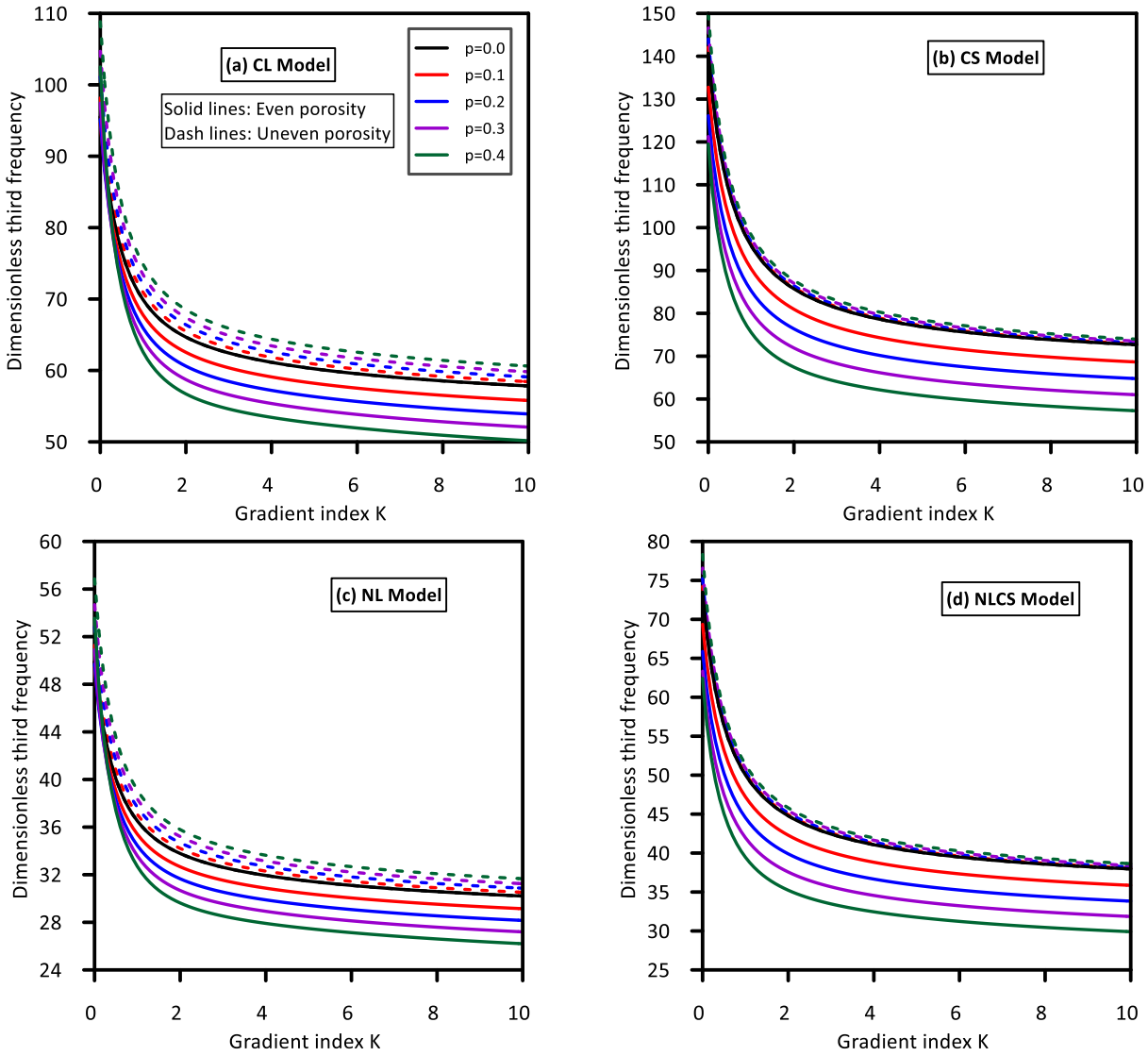

Fig. 8 Variation of the dimensionless third frequency with the gradient index at different porosities using even and uneven porosity models

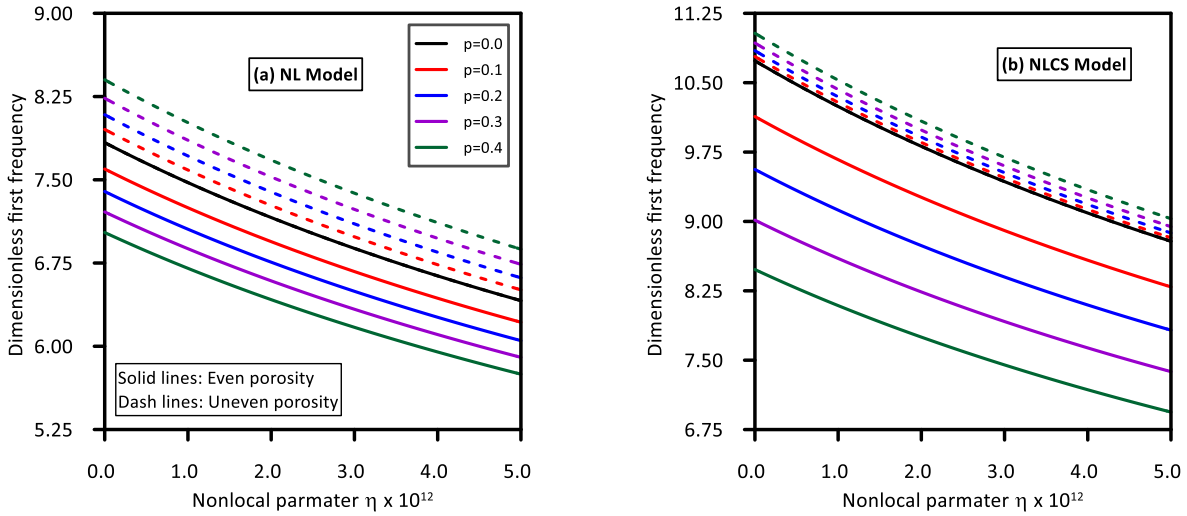

Fig. 9 Variation of the dimensionless first frequency with the nonlocal parameter (η) at different porosities using even and uneven porosity model (K = 1)

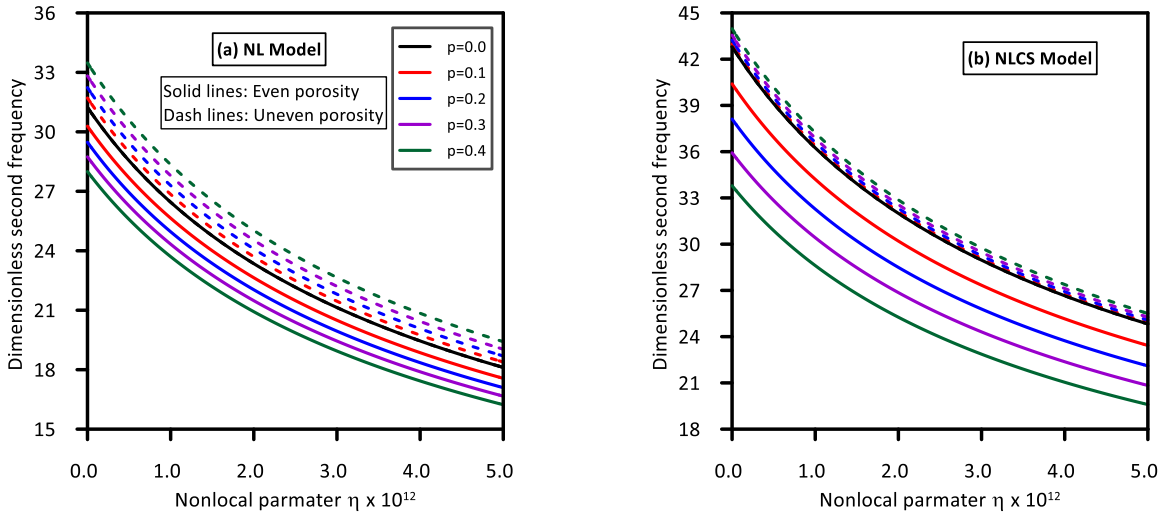

Fig. 10 Variation of the dimensionless second frequency with the nonlocal parameter (η) at different porosities using even and uneven porosity model (K = 1)

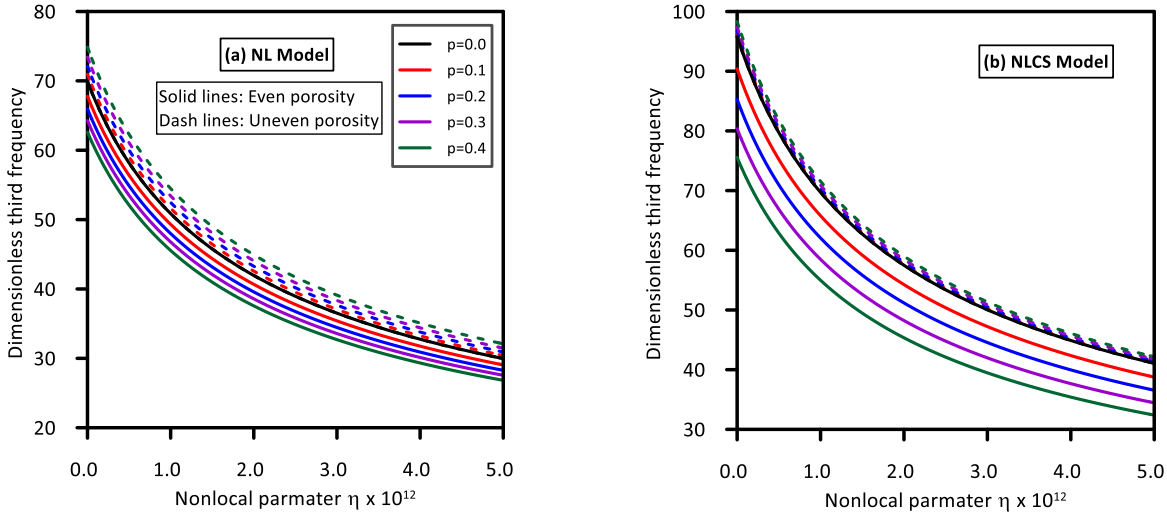

Fig. 11 Variation of the dimensionless third frequency with the nonlocal parameter (η) at different porosities using even and uneven porosity model (K = 1)

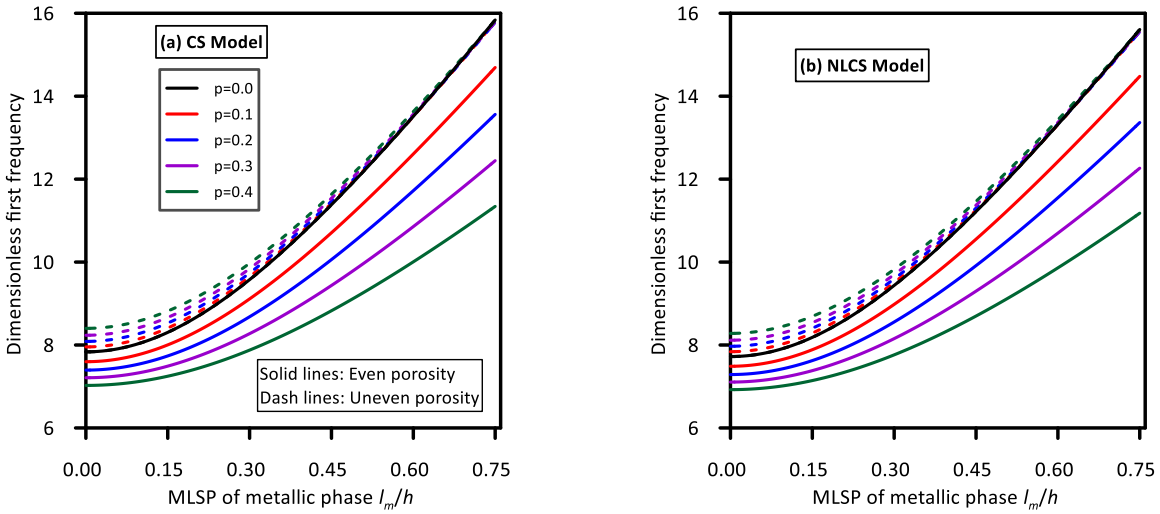

Fig. 12 Variation of the dimensionless first frequency with the dimensionless material length scale parameter (l_m/h) at different porosities using even and uneven porosity model (K = 1)

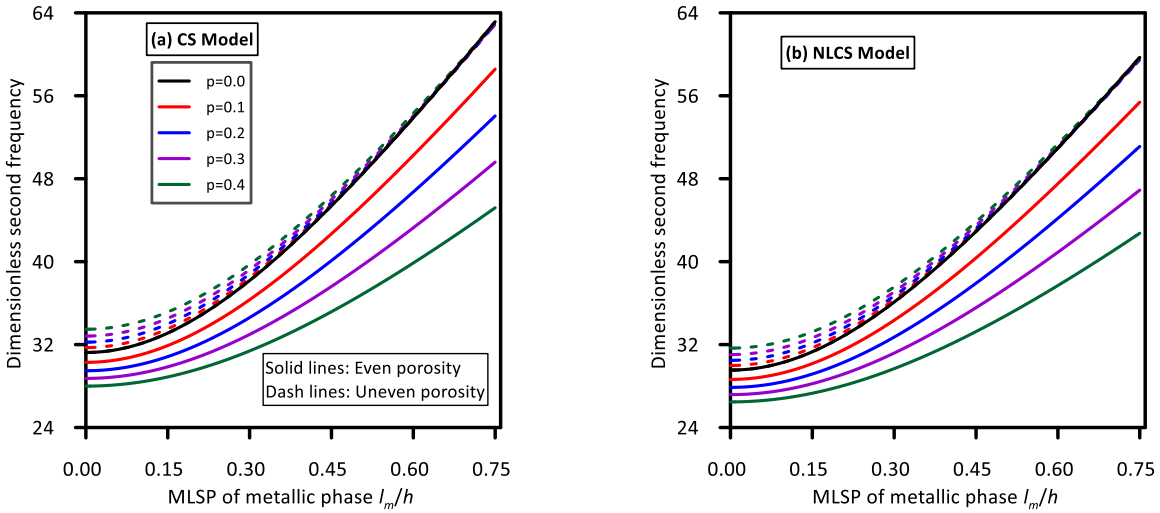

Fig. 13 Variation of the dimensionless second frequency with the dimensionless material length scale parameter (l_m/h) at different porosities using even and uneven porosity model (K = 1)

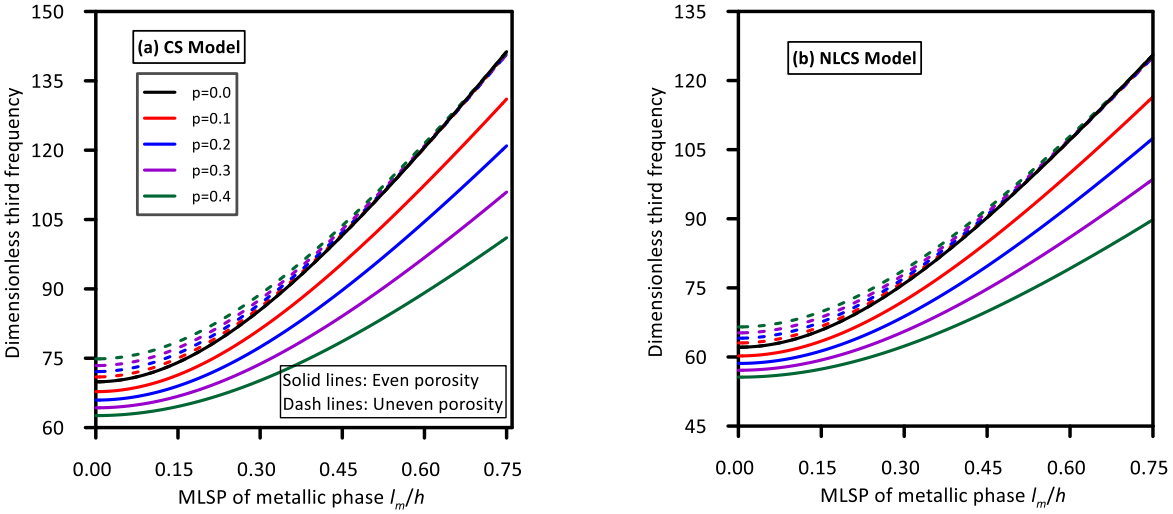

Fig. 14 Variation of the dimensionless third frequency with the dimensionless material length scale parameter (l_m/h) at different porosities using even and uneven porosity model (K = 1)

the power-law exponent K, which is attributed to the increase of the metallic content as K and therefore, the mass and stiffness of the porous FG nanobeam are respectively, increases and decreases. In addition, the contribution of nonlocal parameter is not affected with K, and thus the ratio of the predicted frequencies based on NL model-to-that based on CL model is almost independent of K. The effect of the porosity content based on the CS and NLCS models, is very small compared with that based on the CL and NL models.

The influence of the porosity content at different values of the nonlocal parameter in the framework of NL and NLCS models is illustrated in Figs. 10–12. It is depicted the variations of the first three frequencies with the nonlocal parameter have the same trends for different porosity contents under both even and even types. These constant trends are owing to that the porosity content is not contribute to the nonlocal parameter. Also, as the nonlocal parameter increases, the predicted frequencies considerably decrease due to the stiffness-softening effect introduced by the nonlocality. Additionally, it is noticeable that for all values of the nonlocal parameter, the effect of porosity content for even type is much greater than that of uneven type, epically with the NLCS modelling. Also, the effect of porosity with even and uneven types becomes more pronounced for the NLCS and NL analyses, respectively. Higher modes of vibration results in a lower influence of porosity content on the predicted frequency.

Figs. 13-15 demonstrate the variations of dimensionless first three frequencies of porous FG nanobeam with the ratio of the material length scale parameter-to-thickness (l_m/h) based on the CS and NLCS continuum models. To explore the impact of porosity content and type of distribution, the results are predicted at various porosity parameters using even and uneven distribution of porosities. Interestingly, it is found that for both CS and NLCS models, increasing l_m/h shows the impact of the porosity content increases and decreases for even and uneven types of distribution, respectively. It is shown that the predicted dimensionless frequencies are remarkably increased as l_m/h rises, which is owing to the increased stiffness-hardening effect by increasing l_m/h and thus the beam becomes stiffer. The NLCS model gives lower frequencies than those predicted from the CS model due to the nonlocal softening effect. It is depicted that the nonlocal effect reduces as l_m/h rises.

6. Conclusions

An investigation on post-buckling behavior of FG-MEE cylindrical microshell under mechanical, electrical and magnetic loadings was presented in the article. Mathematical formulation based on strain gradient theory gave a scale coefficient for the description of increase in structural stiffness at microscale. Functionally gradation of material properties was defined according to power-law function. The governing equations were presented in the framework of DQ method and then post-buckling curves were obtained as functions of maximum deflection. It was seen that the buckling load of microshell first reduced with increase of maximum deflection and then it increased. In fact, immediately after the critical buckling load, the microshell had no post-buckling capability and buckling load reduced. Another observation was that post-buckling curves of the microshell were influenced by strain gradient effects. It was also seen that increase of material index led to lower post-buckling loads. Also, as the value of material index was smaller, the post-buckling curves based on various values of applied electric voltage became closer to each other.

Acknowledgement

This project was funded by the Deanship of Scientific Research (DSR) at King Abdulaziz University, Jeddah, under Grant no. G-57-135-1441. The authors, therefore, acknowledge with thanks DSR for technical and financial support.

References

Abdelrahman, A.A. and Eltaher, M.A. (2020), "On bending and buckling responses of perforated nanobeams including surface energy for different beams theories", *Eng. Comput.*, 1-27. https://doi.org/10.1007/s00366-020-01211-8.

Abdelrahman, A.A., Esen, I., Özarpa, C. and Eltaher, M.A. (2021), "Dynamics of perforated nanobeams subject to moving mass using the nonlocal strain gradient theory", *Appl. Math. Model.*, **96**, 215-235. https://doi.org/10.1016/j.apm.2021.03.008.

Abo-Bakr, R.M., Eltaher, M.A. and Attia, M.A. (2020a), "Pull-in and freestanding instability of actuated functionally graded nanobeams including surface and stiffening effects", *Eng. Comput.*, 1-22. https://doi.org/10.1007/s00366-020-01146-0.

Abo-Bakr, H.M., Abo-Bakr, R.M., Mohamed, S.A. and Eltaher, M.A. (2020b), "Weight optimization of axially functionally graded microbeams under buckling and vibration behaviors", *Mech. Based Des. Struct.*, 1-22. https://doi.org/10.1080/15397734.2020.1838298.

Abo-Bakr, R.M., Abo-Bakr, H.M., Mohamed, SA. and Eltaher, M.A. (2021a), "Optimal weight for buckling of FG beam under variable axial load using Pareto optimality", *Compos. Struct.*, **258**, 113193. https://doi.org/10.1016/j.compstruct.2020.113193.

Abo-bakr, H.M., Abo-bakr, R.M., Mohamed, S.A. and Eltaher, M.A. (2021b), "Multi-objective shape optimization for axially functionally graded microbeams", *Compos. Struct.*, **258**, 113370. https://doi.org/10.1016/j.compstruct.2020.113370.

Akbari, H., Azadi, M. and Fahham, H. (2020), "Free vibration analysis of thick sandwich cylindrical panels with saturated FG-porous core", *Mech. Based Des. Struct.*, 1-19. https://doi.org/10.1080/15397734.2020.1748051.

Akbaş, Ş.D., Fageehi, Y.A., Assie, A.E. and Eltaher, M.A. (2020a), "Dynamic analysis of viscoelastic functionally graded porous thick beams under pulse load", *Eng. Comput.*, 1-13. https://doi.org/10.1007/s00366-020-01070-3.

Akbaş, Ş.D., Bashiri, A.H., Assie, A.E. and Eltaher, M.A. (2020b), "Dynamic analysis of thick beams with functionally graded porous layers and viscoelastic support", *J Vib. Control*, 1077546320947302. https://doi.org/10.1177/1077546320947302.

Alazwari, M.A., Abdelrahman, A.A., Wagih, A., Eltaher, M.A. and Abd-El-Mottaleb, H.E. (2021), Static analysis of cutout microstructures incorporating the microstructure and surface

effects. *Steel Compos. Struct.*, **38**(5), 583-597. https://doi.org/10.12989/scs.2021.38.5.583.

Alipour, M.M. and Shariyat, M. (2019), "Nonlocal zigzag analytical solution for Laplacian hygrothermal stress analysis of annular sandwich macro/nanoplates with poor adhesions and 2D-FGM porous cores", *Arch. Civil Mech. Eng.*, **19**(4), 1211-1234. https://doi.org/10.1016/j.acme.2019.06.008.

Alnujaie, A., Akbas, S.D., Eltaher, M.A. and Assie, A. (2021a), "Forced vibration of a functionally graded porous beam resting on viscoelastic foundation", *Geomech. Eng.*, **24**(1), 91-103. https://doi.org/10.12989/gae.2021.24.1.091.

Alnujaie, A., Akbaş, Ş.D., Eltaher, M.A. and Assie, A.E. (2021b), "Damped forced vibration analysis of layered functionally graded thick beams with porosity", *Smart Struct. Syst.*, **27**(4), 679-689. https://doi.org/10.12989/sss.2021.27.4.679.

Alshorbagy, A.E., Eltaher, M.A. and Mahmoud, F.F. (2011), "Free vibration characteristics of a functionally graded beam by finite element method", *Appl. Math. Model.*, **35**(1), 412-425. https://doi.org/10.1016/j.apm.2010.07.006.

Aria, A.I. and Friswell, M.I. (2019), "A nonlocal finite element model for buckling and vibration of functionally graded nanobeams", *Compos. Part B Eng.*, **166**, 233-246. https://doi.org/10.1016/j.compositesb.2018.11.071.

Aria, A.I., Rabczuk, T. and Friswell, M.I. (2019), "A finite element model for the thermo-elastic analysis of functionally graded porous nanobeams", *Eur. J. Mech. A. Solids*, **77**, 103767. https://doi.org/10.1016/j.euromechsol.2019.04.002.

Asemi, K., Babaei, M. and Kiarasi, F. (2020), "Static, natural frequency and dynamic analyses of functionally graded porous annular sector plates reinforced by graphene platelets", *Mech. Based Des. Struct.*, 1-29. https://doi.org/10.1080/15397734.2020.1822865.

Attia, M.A. (2017), "On the mechanics of functionally graded nanobeams with the account of surface elasticity", *Int. J. Eng. Sci.*, **115**, 73-101. https://doi.org/10.1016/j.ijengsci.2017.03.011

Attia, M.A. and Rahman, A.A.A. (2018), "On vibrations of functionally graded viscoelastic nanobeams with surface effects", *Int. J. Eng. Sci.*, **127**, 1-32. https://doi.org/10.1016/j.ijengsci.2018.02.005.

Attia, M.A. and Mohamed, S.A. (2020), "Nonlinear thermal buckling and postbuckling analysis of bidirectional functionally graded tapered microbeams based on Reddy beam theory", *Eng. Comput.*, 1-30. https://doi.org/10.1007/s00366-020-01080-1.

Barati, M.R. (2017), "Nonlocal-strain gradient forced vibration analysis of metal foam nanoplates with uniform and graded porosities", *Adv. Nano Res.*, **5**(4), 393. https://doi.org/10.12989/anr.2017.5.4.393.

Bashiri, A.H., Akbas, S.D., Abdelrahman, A.A., Assie, A., Eltaher, M.A. and Mohamed, E.F. (2021), "Vibration of multilayered functionally graded deep beams under thermal load", *Geomech. Eng.*, **24**(6), 545-557. https://doi.org/10.12989/gae.2021.24.6.545.

Daikh, A.A., Drai, A., Houari, M.S.A. and Eltaher, M.A. (2020), "Static analysis of multilayer nonlocal strain gradient nanobeam reinforced by carbon nanotubes", *Steel Compos. Struct.*, **36**(6), 643-656. https://doi.org/10.12989/scs.2020.36.6.643.

Daikh, A.A., Houari, M.S.A. and Eltaher, M.A. (2021a), "A novel nonlocal strain gradient Quasi-3D bending analysis of sigmoid functionally graded sandwich nanoplates", *Compos. Struct.*, **262**, 113347. https://doi.org/10.1016/j.compstruct.2020.113347.

Daikh, A.A., Houari, M.S.A., Karami, B., Eltaher, M.A., Dimitri, R. and Tornabene, F. (2021b), "Buckling Analysis of CNTRC Curved Sandwich Nanobeams in Thermal Environment", *Appl. Sci.*, **11**(7), 3250. https://doi.org/10.3390/app11073250.

Demirhan, P.A. and Taskin, V. (2019), "Bending and free vibration analysis of Levy-type porous functionally graded plate using state space approach", *Compos. Part B Eng.*, **160**, 661-676. https://doi.org/10.1016/j.compositesb.2018.12.020.

Dong, Y.H., He, L.W., Wang, L., Li, Y.H. and Yang, J. (2018), "Buckling of spinning functionally graded graphene reinforced porous nanocomposite cylindrical shells: an analytical study", *Aerosp. Sci. Technol.*, **82**, 466-478. https://doi.org/10.1016/j.ast.2018.09.037.

Ebrahimi, F. and Salari, E. (2015), "Thermal buckling and free vibration analysis of size dependent Timoshenko FG nanobeams in thermal environments", *Compos. Struct.*, **128**, 363-380. http://doi.org/10.1016/j.compstruct.2015.03.023.

Ebrahimi, F., Ghasemi, F. and Salari, E. (2016), "Investigating thermal effects on vibration behavior of temperature-dependent compositionally graded Euler beams with porosities", *Meccanica*, **51**(1), 223-249. https://doi.org/10.1007/s11012-015-0208-y.

Ebrahimi, F. and Dabbagh, A. (2019), "A novel porosity-based homogenization scheme for propagation of waves in axially-excited FG nanobeams", *Adv. Nano Res.*, **7**(6), 379-390. https://doi.org/10.12989/anr.2019.7.6.379.

Ebrahimi, F., Daman, M. and Mahesh, V. (2019), "Thermo-mechanical vibration analysis of curved imperfect nano-beams based on nonlocal strain gradient theory", *Adv. Nano Res.*, **7**(4), 249-263. https://doi.org/10.12989/anr.2019.7.4.249.

Ebrahimi, F., Jafari, A. and Selvamani, R. (2020), "Thermal buckling analysis of magneto-electro-elastic porous FG beam in thermal environment", *Adv. Nano Res.*, **8**(1), 83-94. https://doi.org/10.12989/anr.2020.8.1.083.

Ebrahimi, F., Seyfi, A., Nouraei, M. and Haghi, P. (2021), "Influence of magnetic field on the wave propagation response of functionally graded (FG) beam lying on elastic foundation in thermal environment", *Wave. Random Complex*, 1-19. https://doi.org/10.1080/17455030.2020.1847359.

Eltaher, M.A., Alshorbagy, A.E. and Mahmoud, F.F. (2013), "Determination of neutral axis position and its effect on natural frequencies of functionally graded macro/nanobeams", *Compos. Struct.*, **99**, 193-201. https://doi.org/10.1016/j.compstruct.2012.11.039.

Eltaher, M.A., Fouda, N., El-midany, T. and Sadoun, A.M. (2018), "Modified porosity model in analysis of functionally graded porous nanobeams", *J. Braz. Soc. Mech. Sci. Eng.*, **40**(3), 1-10. https://doi.org/10.1007/s40430-018-1065-0.

Emdadi, M., Mohammadimehr, M. and Navi, B.R. (2019), "Free vibration of an annular sandwich plate with CNTRC facesheets and FG porous cores using Ritz method", *Adv. Nano Res.*, **7**(2), 109-123. https://doi.org/10.12989/anr.2019.7.2.109.

Eringen, A.C. (1972), "Nonlocal polar elastic continua", *Int. J. Eng. Sci.*, **10**(1), 1-16. https://doi.org/10.1016/0020-7225(72)90070-5.

Eringen, A.C. (1983), "On differential equations of nonlocal elasticity and solutions of screw dislocation and surface waves", *J. Appl. Phys.*, **54**(9), 4703-4710. https://doi.org/10.1063/1.332803.

Esen, I., Eltaher, M.A. and Abdelrahman, A.A. (2021a), "Vibration response of symmetric and sigmoid functionally graded beam rested on elastic foundation under moving point mass", *Mech. Based Des. Struct.*, 1-25. https://doi.org/10.1080/15397734.2021.1904255.

Esen, I., Abdelrhmaan, A.A. and Eltaher, M.A. (2021b), "Free vibration and buckling stability of FG nanobeams exposed to magnetic and thermal fields", *Eng. Comput.*, 1-20. https://doi.org/10.1007/s00366-021-01389-5.

Esen, I., Özarpa, C. and Eltaher, M.A. (2021c), "Free vibration of a cracked FG microbeam embedded in an elastic matrix and exposed to magnetic field in a thermal environment", *Compos. Struct.*, **261**, 113552. https://doi.org/10.1016/j.compstruct.2021.113552.

Esmaeili, M. and Beni, Y.T. (2019), "Vibration and buckling

analysis of functionally graded flexoelectric smart beam", *J. Appl. Comput. Mech*., **5**(5), 900-917. https://doi.org/10.22055/JACM.2019.27857.1439.

Esmaeilzadeh, M., Golmakani, M.E. and Sadeghian, M. (2020), "A nonlocal strain gradient model for nonlinear dynamic behavior of bi-directional functionally graded porous nanoplates on elastic foundations", *Mech. Based Des. Struct*., 1-20. https://doi.org/10.1080/15397734.2020.1845965.

Faleh, N.M., Ahmed, R.A. and Fenjan, R.M. (2018), "On vibrations of porous FG nanoshells", *Int. J. Eng. Sci*., **133**, 1-14. https://doi.org/10.1016/j.ijengsci.2018.08.007.

Fan, F., Cai, X., Sahmani, S. and Safaei, B. (2021), "Isogeometric thermal postbuckling analysis of porous FGM quasi-3D nanoplates having cutouts with different shapes based upon surface stress elasticity", *Compos. Struct*., **262**, 113604. https://doi.org/10.1016/j.compstruct.2021.113604.

Farajpour, A., Rastgoo, A. and Mohammadi, M. (2014), "Surface effects on the mechanical characteristics of microtubule networks in living cells", *Mech. Res. Commun*., **57**, 18-26. http://doi.org/10.1016/j.mechrescom.2014.01.005.

Farzam, A. and Hassani, B. (2019), "Isogeometric analysis of in-plane functionally graded porous microplates using modified couple stress theory", *Aerosp. Sci. Technol*., **91**, 508-524. https://doi.org/10.1016/j.ast.2019.05.012.

Fattahi, A.M., Sahmani, S. and Ahmed, N.A. (2020), "Nonlocal strain gradient beam model for nonlinear secondary resonance analysis of functionally graded porous micro/nano-beams under periodic hard excitations", *Mech. Based Des. Struct*., **48**(4), 403-432. https://doi.org/10.1080/15397734.2019.1624176.

Fenjan, R.M., Moustafa, N.M. and Faleh, N.M. (2020), "Scale-dependent thermal vibration analysis of FG beams having porosities based on DQM", *Adv. Nano Res*., **8**(4), 283-292. https://doi.org/10.12989/anr.2020.8.4.283.

Fouda, N., El-Midany, T. and Sadoun, A.M. (2017), "Bending, buckling and vibration of a functionally graded porous beam using finite elements", *J. Appl. Comput. Mech*., **3**(4), 274-282. https://doi.org/10.22055/JACM.2017.21924.1121.

Ghandourh, E.E. and Abdraboh, A.M. (2020), "Dynamic analysis of functionally graded nonlocal nanobeam with different porosity models", *Steel Compos. Struct*., **36**(3), 293-305. https://doi.org/10.12989/scs.2020.36.3.293.

Hadji, L. and Avcar, M. (2021), "Nonlocal free vibration analysis of porous FG nanobeams using hyperbolic shear deformation beam theory", *Adv. Nano Res*., **10**(3), 281-293. https://doi.org/10.12989/anr.2021.10.3.281.

Hamed, M.A., Sadoun, A.M. and Eltaher, M.A. (2019a), "Effects of porosity models on static behavior of size dependent functionally graded beam", *Struct. Eng. Mech*., **71**(1), 89-98. https://doi.org/10.12989/sem.2019.71.1.089.

Hamed, M.A., Abo-bakr, R.M., Mohamed, S.A. and Eltaher, M.A. (2020), "Influence of axial load function and optimization on static stability of sandwich functionally graded beams with porous core", *Eng. Comput.*, **36**(4), 1929-1946. https://doi.org/10.1007/s00366-020-01023-w.

Hamidi, B.A., Hosseini, S.A., Hayati, H. and Hassannejad, R. (2020), "Forced axial vibration of micro and nanobeam under axial harmonic moving and constant distributed forces via nonlocal strain gradient theory", *Mech. Based Des. Struct*., 1-15. https://doi.org/10.1080/15397734.2020.1744003.

Jalaei, M.H. and Civalek, Ö. (2019), "On dynamic instability of magnetically embedded viscoelastic porous FG nanobeam", *Int. J. Eng. Sci*., **143**, 14-32. https://doi.org/10.1016/j.ijengsci.2019.06.013.

Jena, S.K., Chakraverty, S., Malikan, M. and Tornabene, F. (2019), "Stability analysis of single-walled carbon nanotubes embedded in winkler foundation placed in a thermal environment considering the surface effect using a new refined beam theory", *Mech. Based Des. Struct*., 1-15. https://doi.org/10.1080/15397734.2019.1698437.

Karamanli, A. and Aydogdu, M. (2020), "Structural dynamics and stability analysis of 2D-FG microbeams with two-directional porosity distribution and variable material length scale parameter", *Mech. Based Des. Struct*., **48**(2), 164-191. https://doi.org/10.1080/15397734.2019.1627219.

Kim, J., Żur, K.K. and Reddy, J.N. (2019), "Bending, free vibration, and buckling of modified couples stress-based functionally graded porous micro-plates", *Compos. Struct*., **209**, 879-888. https://doi.org/10.1016/j.compstruct.2018.11.023.

Kitipornchai, S., Chen, D. and Yang, J. (2017), "Free vibration and elastic buckling of functionally graded porous beams reinforced by graphene platelets", *Mater. Des*., **116**, 656-665. http://doi.org/10.1016/j.matdes.2016.12.061.

Koochi, A. and Goharimanesh, M. (2021), "Nonlinear oscillations of CNT nano-resonator based on nonlocal elasticity: The energy balance method", *Rep. Mech. Eng*., **2**(1), 41-50. https://doi.org/10.31181/rme200102041g.

Le, N.L., Nguyen, T.P., Vu, H.N., Nguyen, T.T. and Vu, M.D. (2020), "An analytical approach of nonlinear thermo-mechanical buckling of functionally graded graphene-reinforced composite laminated cylindrical shells under compressive axial load surrounded by elastic foundation", *J. Appl. Comput. Mech*., **6**(2), 357-372. https://doi.org/10.22055/JACM.2019.29527.1609.

Li, L. and Hu, Y. (2016), "Nonlinear bending and free vibration analyses of nonlocal strain gradient beams made of functionally graded material", *Int. J. Eng. Sci*., **107**, 77-97. http://doi.org/10.1016/j.ijengsci.2016.07.011.

Lu, L., She, G.L. and Guo, X. (2021a), "Size-dependent postbuckling analysis of graphene reinforced composite microtubes with geometrical imperfection", *Int. J. Mech. Sci*., **199**, 106428. https://doi.org/10.1016/j.ijmecsci.2021.106428.

Lu, L., Wang, S., Li, M. and Guo, X. (2021b), "Free vibration and dynamic stability of functionally graded composite microtubes reinforced with graphene platelets", *Compos. Struct*., **272**, 114231. https://doi.org/10.1016/j.compstruct.2021.114231.

Lyashenko, I.A., Borysiuk, V.N. and Popov, V.L. (2020), "Dynamical model of the asymmetric actuator of directional motion based on power-law graded materials", *Mech. Eng*., 245-254. https://doi.org/10.22190/FUME200129020L.

Ma, H.M., Gao, X.L. and Reddy, J.N. (2008), "A microstructure-dependent Timoshenko beam model based on a modified couple stress theory", *J. Mech. Phys. Solids*, **56**(12), 3379-3391. https://doi.org/10.1016/j.jmps.2008.09.007.

Mindlin, R.D, (1963), "Influence of couple-stresses on stress concentrations", *Experimental Mechanics*, **3**, 1-7.

Mohammadimehr, M. and Meskini, M. (2020), "Analysis of porous micro sandwich plate: Free and forced vibration under magneto-electro-elastic loadings", *Adv. Nano Res*., **8**(1), 69-82. https://doi.org/10.12989/anr.2020.8.1.069.

Moory-Shirbani, M., Sedighi, H.M., Ouakad, H.M. and Najar, F. (2018), "Experimental and mathematical analysis of a piezoelectrically actuated multilayered imperfect microbeam subjected to applied electric potential", *Compos. Struct*., **184**, 950-960. https://doi.org/10.1016/j.compstruct.2017.10.062.

Reddy, J.N. (2007), "Nonlocal theories for bending, buckling and vibration of beams", *Int. J. Eng. Sci*., **45**(2-8), 288-307. https://doi.org/10.1016/j.ijengsci.2007.04.004.

Reddy, J.N. (2011), "Microstructure-dependent couple stress theories of functionally graded beams", *J. Mech. Phys. Solids*, **59**(11), 2382-2399. https://doi.org/10.1016/j.jmps.2011.06.008.

Sahmani, S. and Madyira, D.M. (2019), "Nonlocal strain gradient nonlinear primary resonance of micro/nano-beams made of GPL reinforced FG porous nanocomposite materials", *Mech. Based Des. Struct*., 1-28.

https://doi.org/10.1080/15397734.2019.1695627
Sedighi, H.M. and Daneshmand, F. (2014), "Static and dynamic pull-in instability of multi-walled carbon nanotube probes by He's iteration perturbation method", *J. Mech. Sci. Technol.*, **28**(9), 3459-3469. https://doi.org/10.1007/s12206-014-0807-x.
Sedighi, H.M., Abouelregal, A.E. and Faghidian, S.A. (2021), "Modified couple stress flexure mechanics of nanobeams", *Physica Scripta*, **96**(11), 115402. https://doi.org/10.1088/1402-4896/ac13e2.
Shariati, A., Mohammad-Sedighi, H., Żur, K.K., Habibi, M. and Safa, M. (2020), "Stability and dynamics of viscoelastic moving rayleigh beams with an asymmetrical distribution of material parameters", *Symmetry*, **12**(4), 586. https://doi.org/10.3390/sym12040586.
She, G.L. (2020), "Wave propagation of FG polymer composite nanoplates reinforced with GNPs", *Steel Compos. Struct.*, **37**(1), 27-35. https://doi.org/10.12989/scs.2020.37.1.027.
She, G.L., Liu, H.B. and Karami, B. (2021), "Resonance analysis of composite curved microbeams reinforced with graphene nanoplatelets", *Thin Wall. Struct.*, **160**, 107407. https://doi.org/10.1016/j.tws.2020.107407.
Şimşek, M. (2016), "Nonlinear free vibration of a functionally graded nanobeam using nonlocal strain gradient theory and a novel Hamiltonian approach", *Int. J. Eng. Sci.*, **105**, 12-27. https://doi.org/10.1016/j.ijengsci.2016.04.013.
Soliman, A.E., Eltaher, M.A., Attia, M.A. and Alshorbagy, A.E. (2018), "Nonlinear transient analysis of FG pipe subjected to internal pressure and unsteady temperature in a natural gas facility", *Struct. Eng. Mech.*, **66**(1), 85-96. http://dx.doi.org/10.12989/sem.2018.66.1.085.
Su, J., Qu, Y., Zhang, K., Zhang, Q. and Tian, Y. (2021), "Vibration analysis of functionally graded porous piezoelectric deep curved beams resting on discrete elastic supports", *Thin Wall. Struct.*, **164**, 107838. https://doi.org/10.1016/j.tws.2021.107838.
Tapia, G., Elwany, A.H. and Sang, H. (2016), "Prediction of porosity in metal-based additive manufacturing using spatial Gaussian process models", *Addit. Manuf.*, **12**, 282-290. https://doi.org/10.1016/j.addma.2016.05.009.
Xu, X., Karami, B. and Shahsavari, D. (2021), "Time-dependent behavior of porous curved nanobeam", *Int. J. Eng. Sci.*, **160**, 103455. https://doi.org/10.1016/j.ijengsci.2021.103455.
Yang, F.A.C.M., Chong, A.C.M., Lam, D.C.C. and Tong, P. (2002), "Couple stress based strain gradient theory for elasticity", *Int. J. Solids Struct.*, **39**(10), 2731-2743. https://doi.org/10.1016/S0020-7683(02)00152-X.
Wattanasakulpong, N. and Ungbhakorn, V. (2014), "Linear and nonlinear vibration analysis of elastically restrained ends FGM beams with porosities", *Aerosp. Sci. Technol.*, **32**(1), 111-120. https://doi.org/10.1016/j.ast.2013.12.002.
Zhang, Y.Y., Wang, Y.X., Zhang, X., Shen, H.M. and She, G.L. (2021), "On snap-buckling of FG-CNTR curved nanobeams considering surface effects", *Steel Compos. Struct.*, **38**(3), 293-304. http://doi.org/10.12989/scs.2021.38.3.293.
Zhu, J., Lai, Z., Yin, Z., Jeon, J. and Lee, S. (2001), "Fabrication of ZrO2–NiCr functionally graded material by powder metallurgy", *Mater. Chem. Phys.*, **68**(1-3), 130-135. https://doi.org/10.1016/S0254-0584(00)00355-2.
Zine, A., Bousahla, A.A., Bourada, F., Benrahou, K.H., Tounsi, A., Adda Bedia, E.A., Mahmoud, S.R. and Tounsi, A. "Bending analysis of functionally graded porous plates via a refined shear deformation theory", *Comput. Concrete*, **26**(1), 63-74. http://doi.org/10.12989/cac.2020.26.1.063.